The Dissertation Committee for Dustin Eldon Lorshbough
certifies that this is the approved version of the following dissertation:

Aspects of Inflationary Cosmology

Committee:

Sonia Paban, Supervisor

Jacques Distler

Willy Fischler

Vadim Kaplunovsky

Natasa Pavlovic

Aspects of Inflationary Cosmology

by

Dustin Eldon Lorshbough, B.S. PHYSICS

DISSERTATION

Presented to the Faculty of the Graduate School of

The University of Texas at Austin

in Partial Fulfillment

of the Requirements

for the Degree of

DOCTOR OF PHILOSOPHY

THE UNIVERSITY OF TEXAS AT AUSTIN

May 2016

Acknowledgments

I would like to thank my family for their unwavering support. The career path from first deciding to enter a Physics undergraduate degree program to obtaining a graduate degree in Physics is filled with uncertainty and I was fortunate to have family members that encouraged me throughout the process.

I would like to thank the faculty, students and staff at the University of Texas for making my experience as a graduate student so pleasant and educational. Jan Duffy was always a welcoming presence within the Theory group and made every morning cheerful. I would also like to thank Abel, Josh and Larry for helping me to navigate through various network issues when they arose.

The guidance from the Theory group faculty was very helpful for understanding current research trends as well as for building a strong foundation in theoretical physics. I especially would like to thank my graduate advisor, Sonia Paban. I was very fortunate to work with Sonia and greatly benefited from her ability to explain physics clearly. I had the great privilege of working on many projects while in graduate school, thanks largely to Sonia's ability to pose or rephrase questions in such a way as to make them answerable. Sonia's patience allowed us to have many deep conversations about both the physics underlying our projects and new research results in the field.

I would like to thank Willy Fischler for many conversations about the relationship between quantum field theory and gravitational phenomena. Willy was very open to discussing new ideas and to exploring project possibilities. This lead to our fruitful collaboration on a wide variety of topics in astrophysics and cosmology. I am grateful for being exposed to his method of thinking about physics.

Though I did not have the opportunity to do projects with other faculty at UT, I still benefited greatly from my interactions with them. I would like to thank Steven Weinberg for teaching me the in-in formalism which played a central role in many of my research contributions. I would like to thank Eiichiro Komatsu for his enthusiastic explanations about relating cosmological theory to observation. I would like to thank Paul Shapiro for organizing the cosmology journal clubs and for fostering a collaborative atmosphere between the physics and astronomy departments. I would like to thank Can Kilic for organizing the phenomenology journal club and LHC results forum from which I learned so much. I would like to thank Jacques Distler for countless clarifying comments and conversations which concisely illuminated the important point of a topic or argument. I would like to thank Vadim Kaplunovsky for very helpful discussions which provided me with a broader context for my research, especially early in my career. I would like to thank Raphael Flauger for discussions on the current trends in cosmology and for helping me to navigate Munich when I visited there for the first time. I would like to thank Elena Caceres for clear and exciting talks on topics in holography.

I would like to thank Greg Sitz for providing guidance during my first exposure to teaching undergraduate courses. I would like to thank Austin Gleeson for discussions about the importance of estimation. I would like to thank John Keto and Matt Ervin for their excellent advice on navigating through the physics degree program.

I would like to thank former Theory group postdocs Pearl Sandick and Ely Kovetz for informing me about possible research topics and paths. I would like to thank the other Theory group postdocs as well for exposing me to new research areas.

I would like to thank my graduate student colleagues for many helpful discussions and collaborations. I would like to thank my officemates Sohaib Alam, Aditya Aravind, Aswin Balasubramanian, Oscar Chacaltana, Jacob Claussen, Anindya Dey and Fei Yan for always creating a pleasant work environment. I am especially indebted to Aditya Aravind for many great collaborations and conversations. I also would like to thank Yingyue Boretz, Dan Carney, Victor Chua, Brandon DiNunno, Stefan Eccles, Jonathan Ganc, Jimmy, Ioannis Keramidas, Matt Klimek, Sandipan Kundu, Rex Lundgren, Juan Pedraza, Tom Mainiero, Joel Meyers, Phuc Nguyen, Ben Stephens, Siva Swaminathan, Walter Tangarife, Andy Trimm, Ben Weaver and Steve Young. The collaborations I had with Dan, Brandon, Stefan, Ben and Walter were very pleasant and productive. I would like to thank Jimmy for an enjoyable collaboration, even though his choice to be mononymous caused disputes with the arXiv moderators.

I am also very grateful to the people that helped me prior to my graduate studies. Though I cannot name them all, there are some faculty at the University of Minnesota that I would like to mention. I would like to thank Cynthia Cattell and John Dombeck for guiding me during my first exposure to publishable research. I would like to thank Yuichi Kubota for his guidance on physics research paths and on choosing a graduate school. I would like to thank Marco Peloso for our discussions on reheating after inflation which foreshadowed what I would pursue during my graduate studies.

The completion of this dissertation was supported by the University of Texas Continuing Fellowship program and by the National Science Foundation under Grant Number PHY-1316033.

Aspects of Inflationary Cosmology

Publication No. _____

Dustin Eldon Lorshbough, Ph.D.
The University of Texas at Austin, 2016

Supervisor: Sonia Paban

We discuss aspects of excited initial states in inflationary cosmology. We review the basic framework of inflationary cosmology and how to compute observable correlation functions. The framework of excited initial states is introduced and the corrections to the cosmological parameters are computed. We show that if the observable modes in the cosmic microwave background are excited, the amplitude of excitation is strongly bounded. We discuss equation of state parameter transitions as a physical mechanism for generating excited initial states. We describe how to interpret the bounds on excitation amplitude as bounds on the parameters of the transition.

Table of Contents

List of Tables

List of Figures

Chapter 1

Introduction

Humanity has pondered the history and structure of our universe long before the tools were developed to study the subject as a precision science [57]. As the physics of general relativity and theory of nucleosynthesis were developed [11, 41, 60, 62, 79] a general picture began to emerge of a universe which was hot at early times, but cooled as space expanded. This basic picture may be formulated as the standard model of cosmology, which states that an early phase of radiation dominated physics lead to a phase dominated by cold dark matter [56, 79]. There is an additional phase which began at very recent times which is dominated by dark energy [58]. It would not be until the early 2000s that precision statements about the parameters of the standard model of cosmology could be made using data from the full sky observations of the cosmic microwave background [32, 36, 44, 72, 74].

It is desirable to understand what physics sets these parameters to have the observed values. The leading paradigm which is capable of explaining the origin of these values is the theory of cosmological inflation [49, 61]. Originally proposed as a way of solving certain cosmological puzzles that arise in big bang cosmology [48, 56], cosmological inflation has provided a framework in

which the tools of quantum field theory may be used to precisely calculate the cosmological parameters [8, 80, 81, 83].

Cosmological inflation is special in that it is a period of accelerated expansion of space. Einstein's theory of General Relativity dictates that in order for there to be an accelerated expansion of space, the energy density occupying that space must be approximately constant. We know that this type of accelerated expansion is possible, because our universe is undergoing a similar type of accelerated expansion today due to dark energy [78].

Our current understanding of the universe is therefore that there was an initial accelerated expansion phase during cosmological inflation, a period of a decelerated expansion due to radiation domination, a period of decelerated expansion due to matter domination and we have now entered a new period of accelerated expansion due to dark energy domination.

We will review the cosmological puzzles and the microscopic description of cosmological inflation in a more quantitative way in the next section. However, it is worth asking if we can ever know what type of phase came before cosmological inflation. Since the cosmic microwave background is the oldest signal which we can observe at present, the question becomes if it is possible to look for imprints of pre-inflationary physics in the cosmic microwave background.

We will show that pre-inflationary signatures are unlikely to comprise the observable cosmic microwave background and therefore we may not probe

pre-inflationary physics. The types of signatures that would necessarily be associated with pre-inflationary physics are too violent to be consistent with observation.

To describe the evolution of cosmological perturbations during the inflationary era we will utilize the well developed framework of quantum field theory in curved spacetime [20, 67, 70]. Despite having a theoretical formalism allowing us to write down models and make predictions, there are basic facts about inflation which are still largely unknown. How inflation came to be within our universe is not known [34, 50, 55, 84]. Furthermore, the duration of inflation has not been well understood [27, 33, 75]. It has been proposed that the transition to inflation may explain observed anomalies in the cosmic microwave background (CMB) if the duration of inflation is not too long [28]. For a discussion of this perspective see [27, 28]. It is within this context that we will show pre-inflationary physics is too violent to be consistent with current observations.

In sections 1.1 and 1.2 we will review the basic motivation and framework of inflationary cosmology. In chapter 2 we will review cosmological perturbation theory and discuss how to compute cosmological observables from the microscopic theory. We will discuss inflationary excited states and how cosmological observables are modified by their presence in chapter 3. We additionally will present bounds on the amplitude of excitation which follow from observational consistency. The mechanism of equation of state transitions for generating excited initial states will be discussed in chapter 4. The bounds

on excitation amplitude will be mapped to bounds on the parameters of the transition. In chapter 5, we conclude.

1.1 Cosmological inflation - cosmological puzzles

There are two generic cosmological puzzles within the framework of standard cosmology which inflation is capable of explaining. One of the puzzles is related to the observed flatness of the universe and is typically referred to as the flatness problem. The other puzzle is related to the observed uniformity of the universe on large scales and is typically referred to as the horizon problem.

An important result is how different components of the universe redshift with the expansion of the universe. The conservation of energy which may be derived from the Einstein field equations takes the form

$$\dot{\rho} + 3H\rho\,(1+w) = 0. \tag{1.1}$$

We have introduced the energy density of the fluid, ρ, the Hubble parameter, H, and the equation of state parameter, $w = P/\rho$, where P is the pressure of the fluid. For dark energy ($w_\Lambda \approx -1$) the energy density is approximately constant. For radiation ($w_{\rm rad} = 1/3$), energy density redshifts as a^{-4}. For matter ($w_{\rm matt} = 0$), energy density redshifts as a^{-3}.

To discuss the flatness puzzle more quantitatively, note that in the presence of 3-curvature the relationship between energy density and geometry is given by [24]

$$\rho = 3M_P^2H^2 + 3M_P^2\frac{k_G}{a^2}. \tag{1.2}$$

We have introduced the reduced Planck mass, $M_P^2 = (8\pi G_N)^{-1} \approx (2.4 \times 10^{18}\ \text{GeV})^2$, and the curvature parameter k_G which may take on any value. If we expand the energy density into the components of radiation, matter and dark energy we obtain the simple relationship

$$\begin{aligned} 1 &= \frac{\rho_{\rm rad}}{3M_P^2H^2} + \frac{\rho_{\rm matt}}{3M_P^2H^2} + \frac{\rho_\Lambda}{3M_P^2H^2} - \frac{k_G}{a^2H^2} \\ &= \frac{H_0^2}{H^2}\left[\frac{\rho_{\rm rad,0}}{3M_P^2H_0^2}\left(\frac{a_0}{a}\right)^4 + \frac{\rho_{\rm matt,0}}{3M_P^2H_0^2}\left(\frac{a_0}{a}\right)^3 + \frac{\rho_\Lambda}{3M_P^2H_0^2} - \frac{k_G}{a_0^2H_0^2}\left(\frac{a_0}{a}\right)^2\right]. \end{aligned} \tag{1.3}$$

In the last line we have chosen to write all time dependence explicitly in terms of the scale factor and the Hubble parameter. In this chapter the 0 subscript denotes the value of the quantity today.

It is customary to rewrite the constant ratio of energy densities in terms of density parameters given by

$$\Omega_{\rm rad,0} = \frac{\rho_{\rm rad,0}}{3M_P^2H_0^2}, \quad \Omega_{\rm matt,0} = \frac{\rho_{\rm matt,0}}{3M_P^2H_0^2}, \quad \Omega_\Lambda = \frac{\rho_{\Lambda,0}}{3M_P^2H_0^2}, \quad \Omega_{\rm curv,0} = -\frac{k_G}{a_0^2H_0^2}. \tag{1.4}$$

This simplifies (1.3) to

$$H^2 = H_0^2\left[\Omega_{\rm rad,0}\left(\frac{a_0}{a}\right)^4 + \Omega_{\rm matt,0}\left(\frac{a_0}{a}\right)^3 + \Omega_{\Lambda,0} + \Omega_{\rm curv,0}\left(\frac{a_0}{a}\right)^2\right]. \tag{1.5}$$

A consistency relation is obtained if we evaluate this expression today,

$$\Omega_{\rm curv,0} = 1 - \Omega_{\Lambda,0} - \Omega_{\rm matt,0} - \Omega_{\rm rad,0}. \tag{1.6}$$

The Planck collaboration [3] has bounded the curvature density parameter using the consistency relation (1.6)

$$\Omega_{\rm curv,0} = 0.0008^{+0.0040}_{-0.0039} \quad (95\%, \text{Planck TT+lowP+lensing+BAO}). \tag{1.7}$$

This implies that the geometry of our universe is consistent with that of a flat universe. The non-vanishing density parameters have been determined to be [3]

$$\Omega_{\rm rad,0} \approx 9 \times 10^{-5}, \quad \Omega_{\rm matt,0} \approx 0.3089, \quad \Omega_{\Lambda} \approx 0.6911. \tag{1.8}$$

Exponential expansion during inflation helps explain why the geometry of our universe is consistent with the geometry of a flat universe. If the curvature density parameter prior to the onset of inflation is given by $\Omega_{\rm curv,init}$, the curvature density parameter today will be

$$\begin{aligned} \Omega_{\rm curv,0} &\approx \Omega_{\rm curv,init} \underbrace{\left(\frac{a_{\rm init}H_{\rm init}}{a_{\rm end}H_{\rm end}}\right)^2}_{H \propto \text{const}} \underbrace{\left(\frac{a_{\rm end}H_{\rm end}}{a_{\rm eq}H_{\rm eq}}\right)^2}_{H \propto a^{-2}} \underbrace{\left(\frac{a_{\rm eq}H_{\rm eq}}{a_0 H_0}\right)^2}_{H \propto a^{-3/2}} . \\ &= \Omega_{\rm curv,init}\, e^{-2N_{\rm tot}+2N_{\rm rad}+N_{\rm matt}} \end{aligned} \tag{1.9}$$

We have approximated the universe after inflation to be radiation dominated and then matter dominated after matter-radiation equality. We have introduced $N_{\rm rad} = \log\left(a_{\rm eq}/a_{\rm end}\right)$ to be the number of efolds between the end of inflation and matter-radiation equality. The number of efolds between matter-radiation equality and today is denoted by $N_{\rm matt} = \log\left(a_0/a_{\rm eq}\right) \approx 8$ [62]. We have introduced $N_{\rm tot} = \log\left(a_{\rm end}/a_{\rm init}\right)$ to denote the total number of efolds of inflation. We see that if the amount of expansion during inflation is greater than amount of expansion after inflation the curvature density parameter will be exponentially suppressed.

The horizon problem is the recognition that points in the sky which are causally disconnected at recombination are very uniform. Consider a mode

which is of the order the horizon size today, $k_{\rm hor} \approx a_0 H_0$. At the end of inflation, the mode would have been far outside of the casual horizon

$$\frac{k_{\rm hor}}{a_{\rm end} H_{\rm end}} = \frac{a_0 H_0}{a_{\rm end} H_{\rm end}} = \left(\frac{a_{\rm eq} H_{\rm eq}}{a_{\rm end} H_{\rm end}}\right)\left(\frac{a_0 H_0}{a_{\rm eq} H_{\rm eq}}\right) = e^{-N_{\rm rad} - N_{\rm matt}/2} \ll 1. \quad (1.10)$$

In order to allow the mode to be within the horizon before the end of inflation, there must be at least $(N_{\rm rad} + N_{\rm matt}/2)$ efolds of inflationary expansion to compensate the post-inflationary expansion. This is similar to the conclusion discussed for solving the flatness problem.

Before leaving this section we will provide an estimate for a lower bound on the duration of inflation if the energy scale of inflation is known.

How many efolds are there between when a mode $k_* = a_* H_*$ exits the horizon during inflation and the end of inflation assuming that reheating after inflation is instantaneous? We compute this directly as [59]

$$\left(\frac{a_{\rm end}}{a_*}\right) = \left(\frac{a_0 H_0}{k_*}\right) \underbrace{\left(\frac{H_*}{H_{\rm end}}\right)}_{\approx 1} \underbrace{\left(\frac{a_{\rm end} H_{\rm end}}{a_{\rm eq} H_{\rm eq}}\right)}_{a \propto H^{-1/2}} \underbrace{\left(\frac{a_{\rm eq} H_{\rm eq}}{a_0 H_0}\right)}_{\approx 43} \approx 43 \left(\frac{a_0 H_0}{k_*}\right)\left(\frac{H_{\rm end}}{H_{\rm eq}}\right)^{1/2}. \quad (1.11)$$

This may be simplified by noting that $H_{\rm eq} \approx (1.6 \times 10^5) H_0 \approx 9.6 \times 10^{-56} M_P$ and that $3 M_P^2 H^2 = \rho$. The number of inflationary efolds from the time the mode exits the horizon until the end of inflation is therefore given by

$$(\Delta N)_* = \log\left(\frac{a_{\rm end}}{a_*}\right) \approx 67 + \frac{1}{4}\log\left(\frac{\rho_{\rm end}}{M_P^4}\right) - \log\left(\frac{k_*}{a_0 H_0}\right). \quad (1.12)$$

Figure 1.1 shows the dependence of the duration on the energy density at the end of inflation. For perspective, note that it takes $(\Delta N)_{\rm CMB} \approx \log(3000) \approx 8$

efolds for all of the modes comprising the observable cosmic microwave background to exit the horizon during inflation.

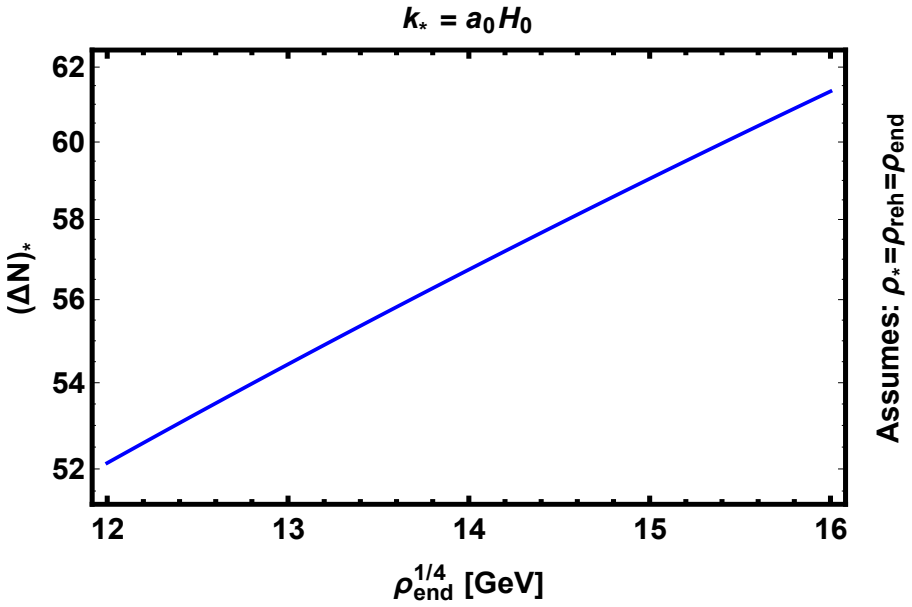

Figure 1.1: The number of inflationary efolds between horizon exit for the mode $k_* = a_0 H_0$ and the end of inflation for various inflationary energy scales.

1.2 Cosmological inflation - microscopic description

The simplest theory for inflation that is consistent with observational data is that of a minimally coupled scalar field [64, 66, 82],

$$S = \int \sqrt{-g} \left[\frac{1}{2} M_P^2 R_S - \frac{1}{2} (\partial\phi)^2 - V \right]. \tag{1.13}$$

We remind the reader that we are using the reduced Planck mass, $M_P^2 = (8\pi G_N)^{-1} \approx (2.4 \times 10^{18} \text{ GeV})^2$. Here R_S is the Ricci scalar, V is the potential energy of the inflaton field and $(\partial\phi)^2$ denotes the usual $g^{\mu\nu}\partial_\mu\phi\,\partial_\nu\phi$. The form

of the Friedmann-Robertson-Walker metric that we will use is given by

$$ds^2 = -dt^2 + a(t)^2 dx^2, \quad \dot{a}(t) = H(t)a(t), \tag{1.14}$$

where $a(t)$ is the cosmic scale factor, $H(t)$ is the Hubble parameter and t is the cosmic time.

We would like to study the connection between the expansion of the universe and the microscopic description of inflation. In order to do so, we need to explicitly write the Einstein field equations. We will first write these equations and then proceed to interpret them.

The Einstein field equations are given as a relation between the Einstein tensor $G_{\mu\nu}$ and the stress-energy tensor $T_{\mu\nu}$ [24],

$$M_P^2 G_{\mu\nu} = T_{\mu\nu}. \tag{1.15}$$

For the Friedmann-Robertson-Walker metric, the Einstein tensor has the non-zero components

$$G_{00} = 3H^2 \text{ and } G_{ij} = -a^2 \left(3H^2 + 2\dot{H}\right) \delta_{ij}. \tag{1.16}$$

The stress-energy tensor for a perfect fluid has the non-zero components

$$T_{00} = \rho \text{ and } T_{ij} = a^2 P \delta_{ij}. \tag{1.17}$$

We have introduced the energy density ρ and pressure P of the fluid. In terms of an inflaton field ϕ, which is approximately homogeneous, $\rho = K + V$ and $P = K - V$. The kinetic energy is $K = \dot{\phi}^2/2$ and V is the potential energy of the inflaton field.

The Einstein equations are given as

$$\rho = 3H^2 M_P^2 \text{ and } -M_P^2\left(3H^2 + 2\dot{H}\right) = P. \tag{1.18}$$

By combining these equations, we obtain the useful relation

$$-\frac{\dot{H}}{H^2} = \frac{3}{2}\left(1 + \frac{P}{\rho}\right) = \frac{3}{2}(1+w) = \epsilon_H. \tag{1.19}$$

We have introduced the equation of state parameter $w = P/\rho$ and the slow-roll parameter ϵ_H. There is another definition of the slow-roll parameter, $\epsilon_\phi = 3K/\rho$, however this is usually equal to ϵ_H so we refer to both as the slow-roll parameter $\epsilon = \epsilon_H = \epsilon_\phi$.

We may rewrite $\dot{H}$ in terms of $\ddot{a}$ in order to make a statement about the expansion of the universe. To obtain an accelerated expansion we require that the parameter ϵ_H be smaller than unity,

$$\ddot{a} = aH^2(1 - \epsilon_H). \tag{1.20}$$

Therefore to produce accelerated expansion the field dynamics must be such that $|\dot{H}| \ll H^2$, or equivalently $K_\phi \ll \rho$. This corresponds to an equation of state parameter which is less than $-1/3$.

The inflaton field excursion during a given number of e-folds may be easily computed as a function of the slow-roll parameter. After changing variables from cosmic time to the number of efolds $dN = Hdt$ we have

$$\epsilon_\phi = \frac{\dot{\phi}^2}{2M_P^2 H^2} \approx \frac{1}{2}\left(\frac{1}{M_P}\frac{d\phi}{dN}\right)^2. \tag{1.21}$$

The field excursion during N inflationary efolds is therefore given by

$$\Delta\phi = \sqrt{2}M_P \int_0^N \sqrt{\epsilon_\phi} dN'. \tag{1.22}$$

For a constant inflationary slow-roll parameter of $\epsilon_\phi \approx 10^{-4}$, 8 efolds of inflation requires an inflaton field excursion of over 11% M_P.

Chapter 2

Primordial observables

Metric perturbations encode information about the physics describing the very early universe. The cosmic microwave background contains signatures from those metric perturbations allowing us to infer the statistical properties of the primordial fluctuations.

We will introduce the perturbed Friedmann-Robertson-Walker metric explicitly in section 2.1 and discuss a convenient gauge to use for the perturbations to the metric in sections 2.2 and 2.3. We will discuss the second and third order action for the scalar and tensor perturbations to the Friedmann-Robertson-Walker metric which will be useful for computing primordial cosmological observables in section 2.4. The in-in formalism for computing cosmological correlation functions will be reviewed in section 2.5 and applied to compute the relevant correlation functions which may currently be probed with observation in section 2.6.

2.1 Metric perturbations

The unperturbed Friedmann-Robertson-Walker metric has already been introduced. It is simply given by

$$ds^2 = a^2 \left(-d\tau^2 + dx^2\right). \tag{2.1}$$

We have introduced τ to represent the conformal time

$$\tau = -\int \frac{dt}{a}. \tag{2.2}$$

We will write the conformal Hubble parameter as

$$\mathcal{H} = \frac{a'(\tau)}{a} = \dot{a}(t). \tag{2.3}$$

There are in principle scalar, vector and tensor perturbations to the metric [64]. The vector perturbations quickly redshift in amplitude during inflation and therefore will be neglected in this study. The tensor perturbations are gauge-independent, so we will wait to discuss them until the end of this section. We may write the scalar perturbations of the metric in a convenient manner as

$$ds^2 = a^2 \left[-e^{2A}d\tau^2 + \left(e^{2B}\right)_{,i} d\tau dx^i + \left(e^{-2R}\delta_{ij} + \left(e^{2E}\right)_{,ij}\right) dx^i dx^j\right]. \tag{2.4}$$

We need to gauge fix because there exists many different coordinate systems capable of describing the same physical spacetime.

The general rules for how quantities change under gauge transformations will be demonstrated for a generic quantity T. In terms of an expansion

in background and fluctuations, we expand T as

$$T = T_0 + \sum_{n=1}^{\infty} \frac{\tilde{\epsilon}}{n!} \delta T_n. \tag{2.5}$$

Here $\tilde{\epsilon}$ denotes a small expansion parameter. Acting with the Lie derivative allows us to transform the quantity T to $\widetilde{T}$

$$\widetilde{T} = e^{\widetilde{\epsilon}\mathcal{L}_\xi} T. \tag{2.6}$$

We match the transformed quantity $\widetilde{T}$ and the original quantity T order by order in $\widetilde{\epsilon}$. Explicitly the expansion becomes

$$\widetilde{T_0} + \widetilde{\epsilon}\widetilde{\delta T_1} + \frac{1}{2}\widetilde{\epsilon}^2 \widetilde{\delta T_2} + \cdots = \left[1 + \widetilde{\epsilon}\mathcal{L}_{\xi_1} + \frac{1}{2}\widetilde{\epsilon}^2 \left(\mathcal{L}_{\xi_1}^2 + \mathcal{L}_{\xi_2}\right)\right] \left[T_0 + \widetilde{\epsilon}\delta T_1 + \frac{1}{2}\widetilde{\epsilon}^2 \delta T_2\right] + \cdots . \tag{2.7}$$

By inspection it may be seen that correspondence between the transformed quantities and the original quantities is

$$\begin{array}{ll} \widetilde{\epsilon}^0: & \widetilde{T_0} = T_0 \\ \widetilde{\epsilon}^1: & \widetilde{\delta T_1} = \delta T_1 + \mathcal{L}_{\xi_1} T_0 \\ \widetilde{\epsilon}^2: & \widetilde{\delta T_2} = \delta T_2 + 2\mathcal{L}_{\xi_1}\delta T_1 + \mathcal{L}_{\xi_1}^2 T_0 + \mathcal{L}_{\xi_2} T_0 \\ & \vdots \end{array} . \tag{2.8}$$

To evaluate the correspondence found in (2.8) more explicitly, we need to be concrete in showing how the Lie derivative acts on tensor quantities. Consider the generating vector

$$\xi_i^\mu = \left(\widetilde{\alpha}_i, \widetilde{\beta}_i, {}^\mu + \widetilde{\gamma}_i^\mu\right), \ \partial_k \widetilde{\gamma}_i^k = 0. \tag{2.9}$$

The i subscript denotes the order of the perturbation. We will only work to leading order so i will always be equal to 1, but in general one must gauge fix

at every order. The action of the Lie derivative on scalar, vector and two-index tensor quantities is then given by contractions of the generating vector with derivatives and the quantities themselves

$$\begin{array}{ll} \text{(Generating Vector)}: & \xi_i^\mu = (\widetilde{\alpha}_i, \beta_i, {}^\mu + \gamma_i^\mu)\,,\ \partial_k \gamma_i^k = 0 \\ \text{(scalars)}: & \mathcal{L}_{\xi_i}\varphi = \xi_i^\lambda \varphi_{,\lambda} \\ \text{(vectors)}: & \mathcal{L}_{\xi_i} v_\mu = \xi_i^\lambda v_{\mu,\lambda} + \xi_{i,\mu}^\alpha v_\alpha \\ \text{(tensors)}: & \mathcal{L}_{\xi_i} t_{\mu\nu} = \xi_i^\lambda t_{\mu\nu,\lambda} + \xi_{i,\nu}^\lambda t_{\mu\lambda} + \xi_{i,\mu}^\lambda t_{\lambda\nu} \end{array} . \tag{2.10}$$

The transformed metric perturbations are now easily obtained. Consider the (00) component of the perturbed metric. The transformed quantity is related to the original quantity by

$$\widetilde{\delta g_{00}} = \delta g_{00} + \mathcal{L}_{\xi_1} g_{00} = \delta g_{00} + \xi_1^\lambda g_{00,\lambda} + 2\xi_{1,0}^\lambda g_{0\lambda}. \tag{2.11}$$

Substitution of the generating vector allows us to obtain the transformation rule for the perturbed metric parameter A to leading order

$$\widetilde{A} = A + \widetilde{\alpha}_1 \mathcal{H} + \widetilde{\alpha}_1'. \tag{2.12}$$

We obtain the transformation rules for the perturbed metric parameter B in a similar fashion. We will first write the transformed (0i) component of the metric in terms of the original component

$$\widetilde{\delta g_{0i}} = \delta g_{0i} + \mathcal{L}_{\xi_1} g_{0i} = \delta g_{0i} + \xi_{1,i}^\lambda g_{0\lambda} + \xi_{1,0}^\lambda g_{\lambda i}. \tag{2.13}$$

Substitution of the generating vector yields

$$\widetilde{B} = B - \widetilde{\alpha}_1 + \widetilde{\beta}_1'. \tag{2.14}$$

The behavior of the final two parameters R and E are found by considering the transformation to the (ij) component of the metric

$$\widetilde{\delta g_{ij}} = \delta g_{ij} + \mathcal{L}_{\xi_1} g_{ij} = \delta g_{ij} + \xi_1^\lambda g_{ij,\lambda} + \xi_{1,j}^\lambda g_{i\lambda} + \xi_{1,i}^\lambda g_{\lambda j}. \tag{2.15}$$

In terms of R and E we find

$$\widetilde{R}\delta_{ij} + \widetilde{E}_{,ij} = R\delta_{ij} + E_{,ij} - \widetilde{\alpha}_1 \mathcal{H}\delta_{ij} + \widetilde{\beta}_{1,ij}. \tag{2.16}$$

At the beginning of this section we said that the tensor perturbation is gauge-independent. What that means is that the tensor perturbation does not depend on the choices of α and β in the generating vector,

$$\widetilde{h}_{\rm ij} = h_{\rm ij}. \tag{2.17}$$

2.2 Comoving gauge

A particularly useful gauge to work in is the comoving gauge [64, 82]. The comoving curvature perturbation is known to be conserved outside of the horizon for adiabatic fluctuations, allowing it to encode information from the inflationary era until horizon re-entry. The comoving curvature perturbation is best understood as a constraint on the velocity. We will develop this understanding in this section and relate it to the microscopic inflaton field dynamics in the next section.

The four-velocity of matter is defined with respect to the proper time comoving with the fluid

$$u^\mu = \frac{dx^\mu}{d\tau_{\rm prop}} = \frac{dx^0}{d\tau_{\rm prop}} \left\{1, v^i\right\}, \quad u_\mu u^\mu = -1. \tag{2.18}$$

We have introduced the three-velocity of the matter with respect to the spatial coordinates,

$$v^i = \frac{dx^i}{d\tau}. \tag{2.19}$$

The proper time in terms of three-velocity is given by

$$d\tau^2_{\text{prop}} = a^2\, d\tau^2 \left[1 + 2A - 2B_{,i}v^i - \left(e^{-2R}\delta_{ij} + \left(e^{2E}\right)_{,ij}\right) v^i v^j\right]. \tag{2.20}$$

Note we are going to focus on perfect fluids meaning there exists a locally inertial co-moving frame such that v^i is small [82].

To leading order, the four-velocity components are given by [64]

$$u^0 = \frac{1}{a}\left(1 - A\right), \quad u^i = \frac{1}{a}v^i, u_0 = -a(1 + A), \quad u_i = a(v_i + B_{,i}). \tag{2.21}$$

Lastly, we will need to know how the four-velocity behaves under a gauge transformation. As before,

$$\widetilde{\delta u_i} = \delta u_i + \mathcal{L}_{\xi_1} u_i = \delta u_i + \xi_1^\lambda u_{i,\lambda} + \xi^\lambda_{1,i} u_\lambda. \tag{2.22}$$

Explicitly in terms of the three-velocity this becomes

$$\widetilde{(v_i + B_{,i})} = (v_i + B_{,i}) - \widetilde{\alpha}_{1,i}. \tag{2.23}$$

Having introduced the four-velocity and shown explicitly how it relates to metric perturbations and the three-velocity, we are now ready to define the comoving gauge. The comoving gauge is the coordinate choice corresponding to vanishing matter three-velocity with respect to spatial coordinates. Explicitly we may write

$$\text{Condition 1: } \widetilde{v}_i = 0, \quad \text{Condition 2: } \widetilde{u}_i = 0. \quad \text{(comoving gauge)} \tag{2.24}$$

From our expression for the four-velocity (2.21) we immediately obtain that $\widetilde{B}_{,i} = 0$ as well. We can write the conditions in terms of the generating vector parameters α and β using (2.14) and (2.23). The parameters $\widetilde{\alpha}_{1,\mathrm{com}}$ and $\widetilde{\beta}_{1,\mathrm{com}}$ are given by

$$\left\{ \begin{array}{c} \widetilde{\alpha}_{1,\mathrm{com},i} = (v_i + B_{,i}) \\ \widetilde{\beta}'_{,\mathrm{com},i} = \widetilde{\alpha}_{,\mathrm{com},i} - B_{,i} = v_i \end{array} \right\} \rightarrow \left\{ \begin{array}{c} \widetilde{\alpha}_{1,\mathrm{com}} = (v + B) \\ \widetilde{\beta}'_{1,\mathrm{com}} = \widetilde{\alpha}_{1,\mathrm{com}} - B = v \end{array} \right\}. \qquad (2.25)$$

We have defined a scalar potential v such that $v^i = \delta^{ij} v_{,j} + v^i_{\mathrm{vec}}$, where the divergence of v^i_{vec} vanishes.

The scalar curvature perturbation may now be written in the comoving gauge as

$$\mathcal{R} = \widetilde{R}_{\mathrm{com}} = R - \widetilde{\alpha}_{1,\mathrm{com}} \mathcal{H} = R - aH(v + B). \qquad (2.26)$$

There are many forms of $\mathcal{R}$ used in the literature which are equivalent to this form. In the next section we will list these forms and show explicitly their equivalence.

2.3 Comoving gauge scalar curvature perturbation

There are four commonly used and equivalent forms of the comoving curvature perturbation which we will show to be equivalent if only a single field is present. These forms express $\mathcal{R}$ explicitly in terms of either the velocity perturbation v, the metric perturbation A, the inflaton field perturbation $\delta\phi$ or the Muhkanov-Sasaki variable for the inflaton δQ_ϕ. Note, here we will address the case of a single inflaton field contributing significantly to $\mathcal{R}$. There are multi-field generalizations which easily follow from similar arguments [39, 43,

46, 77]. The four forms of $\mathcal{R}$ are [64]

$$\mathcal{R} \equiv \widetilde{R}_{\rm com} = \begin{cases} R - aH(v+B) & \text{(velocity perturbation)} \\ R - \dfrac{H^2(A + H^{-1}\dot{R})}{\dot{H}} & \text{(metric perturbation)} \\ R + \dfrac{H}{\dot{\phi}}\delta\phi & \text{(field perturbation)} \\ \dfrac{H}{\dot{\phi}}\,\delta Q_\phi & \text{(Muhkanov-Sasaki variable)} \end{cases} \tag{2.27}$$

We will begin by showing the equivalence between the velocity perturbation form and the metric perturbation form. The approach we will take is to consider the perturbed (0i) Einstein field equations

$$\int dx^i M_P^2 \delta G_{0i} = \int dx^i \delta T_{0i}. \tag{2.28}$$

It will be useful to recall that from the background Einstein field equations (1.18) we obtain

$$(\rho + P) = -2M_P^2 \dot{H}. \tag{2.29}$$

We already have introduced the perturbed metric, allowing us to easily obtain the perturbed Einstein tensor. Likewise, the perturbed four-velocity allows us to write the perturbed stress-energy tensor if we note that for a perfect fluid

$$T_{\mu\nu} = (\rho + P)u_\mu u_\nu + P g_{\mu\nu}. \tag{2.30}$$

The result is

$$2M_P^2 \left(\dot{R} + HA\right) = (-a)(\rho + P)(v + B). \tag{2.31}$$

To more easily match the desired form we write

$$aH(v+B) = 2aHM_P^2 \frac{H(A + H^{-1}\dot{R})}{(-a)(\rho + P)} = \frac{H^2(A + H^{-1}\dot{R})}{\dot{H}}. \tag{2.32}$$

This concludes showing the equivalence between the velocity perturbation form and the metric perturbation form.

We will now show the equivalence between the velocity perturbation form and the field perturbation form. To proceed, we write the (0i) component of the perturbed stress energy tensor in terms of both the velocity perturbation as well as explicitly for the inflaton field. For the (0i) component we obtain

$$\delta T_{0i} = (-a)(\rho + P)(v_{,i} + B_{,i}) = \dot{\phi}\delta\phi_{,i}. \tag{2.33}$$

The desired form is easily seen by rewriting this as

$$aH(v + B) = -\frac{H}{\dot{\phi}}\delta\phi. \tag{2.34}$$

This concludes showing the equivalence between the velocity perturbation form and the field perturbation form.

The last step is to show the equivalence between the field perturbation form and the Muhkanov-Sasaki variable form. The Muhkanov-Sasaki variable is the inflaton field perturbation in the flat gauge. Recall that the general transformation rule for a four-scalar which has a homogeneous background component is given by

$$\widetilde{\delta\phi} = \delta\phi + a\,\widetilde{\alpha}\,\dot{\phi}. \tag{2.35}$$

The conditions for the flat gauge are that the spatial metric perturbations vanish,

$$\text{Condition 1: } \widetilde{R} = 0, \quad \text{Condition 2: } \widetilde{E} = 0. \quad \text{(flat gauge)} \tag{2.36}$$

It may be easily shown that this implies that the α and β parameters in the generating vector are given by

$$\widetilde{\alpha}_{1,\text{flat}} = \frac{R}{aH}, \quad \widetilde{\beta}_{1,\text{flat}} = -E. \tag{2.37}$$

The Muhkanov-Sasaki variable is therefore given by

$$\delta Q_\phi = \widetilde{\delta\phi}_{\text{flat}} = \delta\phi + \frac{R}{H}\dot{\phi}. \tag{2.38}$$

It is clear that we recover the field perturbation form by rescaling the Muhkanov-Sasaki variable

$$\frac{H}{\dot{\phi}}\delta Q_\phi = R + \frac{H}{\dot{\phi}}\delta\phi. \tag{2.39}$$

This concludes our demonstration that the field perturbation form is equivalent to the Muhkanov-Sasaki variable form.

We have introduced four different forms for the comoving curvature perturbation which are all equivalent if only a single field is present. For the remainder of this study we will work directly with the comoving curvature perturbation itself, beginning with a review of the second and third order action in the next section.

2.4 $\mathcal{R}$ and h action

We have motivated the comoving curvature perturbation and related it the generic scalar perturbations of the Friedmann-Robertson-Walker metric. In order to compute cosmological observables we must introduce the action for the scalar perturbations.

We will compute two and three point functions of the comoving curvature perturbation, therefore we need the quadratic and cubic action. The standard derivations of these actions are long and involved [63]. We will not be using a modification of these actions, so we will simply state the results and emphasize a redefinition that arises in the cubic action derivation which is necessary to understand the computation of the scalar bispectrum later in this study.

The theory that we will take as our starting pointing is still that of a minimally coupled scalar field in a Friedmann-Robertson-Walker geometry [64, 82]

$$S = \int \sqrt{-g}\left[\frac{1}{2}M_P^2 R_S - \frac{1}{2}(\partial\phi)^2 - V\right], \quad ds^2 = -dt^2 + a^2 dx^2. \tag{2.40}$$

The perturbed quadratic action in terms of the comoving curvature perturbation is given by [63]

$$S_{\mathcal{R}} = -M_P^2 \int \sqrt{-g}\,\epsilon\,(\partial\mathcal{R})^2. \tag{2.41}$$

We will use this quadratic action to compute the primordial scalar power spectrum and the bispectrum later in this study.

The cubic action in terms of $\mathcal{R}$ is involved to write down and will not be directly used so reader is directed to see equation (3.9) of [63] if they wish to see the explicit form. We instead will use a much simpler form by performing a redefinition of $\mathcal{R}$ as originally suggested by [63],

$$\mathcal{R} = \mathcal{R}_c + \left[-\frac{1}{2}\eta + \frac{1}{4}\epsilon\right]\mathcal{R}_c^2 + \frac{1}{2}\epsilon\,\partial^{-2}\left(\mathcal{R}_c\partial^2\mathcal{R}_c\right) + \cdots. \tag{2.42}$$

The cubic action now has the form [63]

$$S_{3,\mathcal{R}} = 4\epsilon^2 H M_P^2 \int d^4x a^5 \dot{\mathcal{R}}_c^2 \left(\partial^{-2}\dot{\mathcal{R}}_c\right) = 4\epsilon^2 H M_P^2 \int d^3x d\tau a^3 \mathcal{R}_c'^2 \left(\partial^{-2}\mathcal{R}_c'\right). \tag{2.43}$$

The advantage of this form is that the three point function in the bispectrum computation that we will perform later is greatly simplified.

Primordial tensor modes have not yet been detected. Therefore it is sufficient to only consider the two point function of tensor perturbations at present. The quadratic action for the tensor perturbations is given by [63]

$$S_h = -\frac{M_P^2}{8} \int \sqrt{-g}\, (\partial h)^2. \tag{2.44}$$

This action will be used to compute the primordial tensor power spectrum later in this study.

2.5 Evaluating correlation functions

In the next section we will relate the cosmological parameters which are probed by observation to correlation functions of the comoving curvature perturbation and the tensor perturbation. However, we will first discuss how one computes correlation functions in cosmology using the in-in formalism.

The in-in formalism is similar to the in-out formalism in usual quantum field theory [22, 80]. The primary difference is that one considers two asymptotically free in states as opposed to an asymptotically free out state. This in practice means that the unitary operator associated with the ket vacuum takes

the same form as in the in-out formalism, but the unitary operator associated with the bra vacuum is switched to an anti-time ordering operator. Explicitly in terms of the time ordering operator T we obtain [8, 80]

$$\langle \mathcal{O}(t) \rangle = \langle 0 | \left(T e^{-i \int_{\infty(1+i\epsilon)}^{t} H_{\rm int}(t') dt'} \right)^{\dagger} \hat{\mathcal{O}}(t) \left(T e^{-i \int_{\infty(1+i\epsilon)}^{t} H_{\rm int}(t') dt'} \right) | 0 \rangle. \quad (2.45)$$

Here $H_{\rm int}$ is the interaction Hamiltonian which may be obtained from a Legendre transformation of the interaction Lagrangian. Just as there are multiple orders of the interaction Lagrangian (corresponding to the quadratic action, cubic action, etc...), there are multiple orders of the interaction Hamiltonian. We have explicitly written the $i\epsilon$ prescription to emphasize that we are considering two asymptotically free in states.

Contributions to the correlation function are obtained by Taylor expanding the exponentials appearing in (2.45). For the purposes of cosmological observables which may presently be probed observationally, we are interested in the two and three point correlation functions. The two point function has a non-vanishing contribution without any insertions of the interaction Hamiltonian, but the three point function requires at least one factor of the interaction Hamiltonian to be non-vanishing. It is possible to organize these expansions in terms of diagrams, but we will only work at leading order so this machinery is not necessary.

In the next section we will explicitly compute the correlation functions relevant for the primordial power spectra and give the current observational results for the cosmological parameters.

2.6 Cosmological observables

Cosmological observables are obtained by computing correlation functions of gauge invariant fluctuations. We will work in the comoving gauge. The quadratic action for the comoving curvature perturbation has already been introduced and is given by

$$S_{\mathcal{R}} = -M_P^2 \int \sqrt{-g}\, \epsilon\, (\partial \mathcal{R})^2. \tag{2.46}$$

Likewise, the quadratic action for the tensor perturbations has already been introduced and may be written as

$$S_h = -\frac{M_P^2}{8} \int \sqrt{-g}\, (\partial h)^2. \tag{2.47}$$

In order to compute quantum correlation functions we promote the spatial fields $\mathcal{R}(\vec{x}, t)$ and $h_{ij}(\vec{x}, t)$ to operators. The vacuum of lowest energy density is defined as a zero particle state in Fock space for all momenta values [67]. Therefore we must Fourier expand the spatial field operators in terms of creation and annihilation operators for each momentum value. In this chapter we will discuss only unexcited states, whereas in the next chapter will introduce excited states.

The comoving curvature perturbation spatial field operator is Fourier expanded in terms of a momentum space field operator as

$$\hat{\mathcal{R}} = \int \frac{d^3k}{(2\pi)^3}\, \hat{\mathcal{R}}_{\vec{k}}\, e^{i\vec{k}\cdot\vec{x}}. \tag{2.48}$$

However, we still must relate the momentum space field operator to the creation and annihilation operators alluded to previously. This is accomplished by introducing the mode function for the field operator, $\mathcal{R}_k$,

$$\hat{\mathcal{R}}_{\vec{k}} = \mathcal{R}_k \, \hat{a}^{\dagger}_{\vec{k}} + \mathcal{R}^*_k \, \hat{a}_{-\vec{k}}. \tag{2.49}$$

The mode functions satisfy the classical equation of motion

$$\ddot{\mathcal{R}}_k + \left(3H + \frac{\dot{\epsilon}}{\epsilon}\right) \dot{\mathcal{R}}_k + \frac{k^2}{a^2} \mathcal{R}_k = 0. \tag{2.50}$$

Usually the $\dot{\epsilon}$ term is absent from the analysis since in the slow-roll approximation it is assumed to be small. However, we will later study transitions which have a large $(\dot{\epsilon}/H\epsilon)$ term and therefore we will keep the term. In the absence of this term the solution of lowest energy density is referred to as the Bunch-Davies solution and is given by [63]

$$\mathcal{R}_{k,BD} = \frac{1}{\sqrt{2\,\epsilon}} \frac{H}{M_P \sqrt{2\,k^3}} \left(1 + i \frac{k}{a\,H}\right) e^{-ik/aH}. \tag{2.51}$$

The normalization of the mode functions is set by the canonical commutation relation. We will verify that the Bunch-Davies solution previously stated (2.51) is properly normalized. The equal time canonical commutation relation is given by the commutator of the field operator with the conjugate momentum

$$\langle 0| \left[\hat{\mathcal{R}}(\vec{x}), \hat{\Pi}_{\mathcal{R}}(\vec{y})\right] |0\rangle = i(2\pi)^3 \delta^3 \left(\vec{x} - \vec{y}\right) \text{ with } \Pi_{\mathcal{R}} = \frac{\partial \mathcal{L}}{\partial \dot{\mathcal{R}}} = 2a^3 \, M_P^2 \, \epsilon \, \dot{\mathcal{R}}. \tag{2.52}$$

We may proceed to Fourier expand the field operators as we have previously discussed

$$2a^3 M_P^2 \epsilon \int \frac{d^3k}{(2\pi)^3} \int \frac{d^3p}{(2\pi)^3} e^{i\vec{k}\cdot\vec{x}} e^{i\vec{p}\cdot\vec{y}} \langle 0| \left[\hat{\mathcal{R}}_{\vec{k}}, \dot{\hat{\mathcal{R}}}_{\vec{p}}\right] |0\rangle = i(2\pi)^3 \delta^3 \left(\vec{x} - \vec{y}\right). \quad (2.53)$$

At this point it is convenient to recall the commutation relation between creation and annihilation operators in quantum field theory is given by

$$\left[\hat{a}_k, \hat{a}^\dagger_{k'}\right] = (2\,\pi)^3 \delta^3 \left(\vec{k} - \vec{k}'\right). \quad (2.54)$$

This allows us to obtain the simple expression which is sometimes referred to as the Wronskian condition

$$2a^3 M_P^2 \epsilon \left(\mathcal{R}^*_k \dot{\mathcal{R}}_k - \mathcal{R}_k \dot{\mathcal{R}}^*_k\right) = i. \quad (2.55)$$

Direct substitution of (2.51) verifies this to be true and therefore the solution is properly normalized.

We will now address the tensor perturbation case. The field operator may be Fourier expanded in terms of a momentum space field operator similar to as was done for the comoving curvature perturbation. The only added complication will be the introduction of the helicity tensors[1] $\epsilon^s_{\vec{k},ij}$,

$$\hat{h}_{ij} = \int \frac{d^3k}{(2\pi)^3} \sum_{s=\pm} \epsilon^s_{k,ij}\, \hat{h}^s_{\vec{k}}\, e^{i\vec{k}\cdot\vec{x}}. \quad (2.56)$$

[1]We work in the helicity basis and therefore the helicity tensors satisfy [18]: $\epsilon^{s=\pm 2}_{\vec{k},ij} = \sqrt{2}\, \epsilon^{s/2}_{\vec{k},i}\, \epsilon^{s/2}_{\vec{k},j}$.

Analogously to the comoving curvature perturbation case we may expand the momentum space field operator in terms of creation and annihilation operators by introducing the mode function h_k^s

$$\hat{h}_{\vec{k}}^s = h_k^s \, \hat{b}_{\vec{k}}^{s\dagger} + h_k^{*s} \, \hat{b}^s{}_{-\vec{k}}. \tag{2.57}$$

The commutation relation satisfied by the creation and annihilation operators is given as

$$\left[\hat{b}_k^s, \hat{b}_{k'}^{s'\dagger}\right] = (2\,\pi)^3 \delta^3 \left(\vec{k} - \vec{k}'\right) \delta^{s,s'}. \tag{2.58}$$

The classical equation of motion satisfied by the tensor perturbation mode function is

$$\ddot{h}_k^s + 3H\dot{h}_k^s + \frac{k^2}{a^2} h_k^s = 0, \tag{2.59}$$

Note the absence of the $\dot{\epsilon}/\epsilon$ term which was present for the comoving curvature perturbation. Later in this study we will show how that term can lead to a large enhancement of the scalar mode function, but a similar enhancement will not occur for the tensor fluctuations.

The solution of lowest energy density for the tensor perturbations is given by

$$h_{k,BD}^s = \sqrt{2} \frac{H}{M_P \sqrt{2\,k^3}} \left(1 + i \frac{k}{a\,H}\right) e^{-ik/aH}. \tag{2.60}$$

It may be verified using the canonical commutation relation for the tensor perturbation that this solution is properly normalized.

The scalar power spectrum has been measured to great accuracy, while the scalar bispectrum and tensor power spectrum have not yet been detected

[5]. The scalar power spectrum is typically parameterized by an amplitude A_s and a scale dependence n_s [5],

$$\langle \hat{\mathcal{R}}_{\vec{k}} \hat{\mathcal{R}}_{\vec{k}'} \rangle = (2\pi)^3 \delta^3 \left(\vec{k} + \vec{k}' \right) P_{\mathcal{R}}(k), \quad \Delta^2_{\mathcal{R}}(k) = \frac{k^3}{2\pi^2} P_{\mathcal{R}}(k) = A_s \left(\frac{k}{k_*} \right)^{n_s - 1 + \mathcal{O}(dn_s/dk)} . \tag{2.61}$$

Similarly, the tensor power spectrum is parameterized by the ratio r of its amplitude to the scalar power spectrum amplitude and a scale dependence n_t [5],

$$4\langle \hat{h}^s_{\vec{k}} \hat{h}^s_{\vec{k}'} \rangle = (2\pi)^3 \delta^3 \left(\vec{k} + \vec{k}' \right) P_t(k), \quad \Delta^2_t(k) = \frac{k^3}{2\pi^2} P_t(k) = (r A_s) \left(\frac{k}{k_*} \right)^{n_t + \mathcal{O}(dn_t/dk)} . \tag{2.62}$$

The scalar bispectrum is typically parameterized by an amplitude f_{NL} and a shape dependence,

$$\langle \hat{\mathcal{R}}_{\vec{k}_1} \hat{\mathcal{R}}_{\vec{k}_2} \hat{\mathcal{R}}_{\vec{k}_3} \rangle = (2\pi)^3 \delta^3 \left(\vec{k}_1 + \vec{k}_2 + \vec{k}_3 \right) B_{k_1, k_2, k_3}. \tag{2.63}$$

$$B_{k_1,k_2,k_3} = \frac{6}{5} f_{\rm NL} \left[P_{\mathcal{R}}(k_1) P_{\mathcal{R}}(k_2) + P_{\mathcal{R}}(k_2) P_{\mathcal{R}}(k_3) + P_{\mathcal{R}}(k_3) P_{\mathcal{R}}(k_1) \right]. \tag{2.64}$$

Three shape templates which are useful for reporting observational results [2, 4, 19] are the equilateral template ($k_1 \approx k_2 \approx k_3$), the folded template ($k_1 \approx k_2 \approx k_3/2$) and the local template ($k_1 \approx k_2 \gg k_3$ in the squeezed limit). A linear combination of the equilateral and folded template is used as opposed to the folded template alone in order to report three statistically independent f_{NL} values [76]. These bispectrum templates are related to their corresponding

$f_{\rm NL}$ values by [2, 19]

$$B_k^{\rm folded} \approx \frac{6}{5} f_{\rm NL}^{\rm fold} \left[P_{\mathcal{R}}(k) P_{\mathcal{R}}(k) + 2 P_{\mathcal{R}}(k) P_{\mathcal{R}}(k/2) \right], \tag{2.65}$$

$$B_k^{\rm equil} \approx \frac{18}{5} f_{\rm NL}^{\rm equil} P_{\mathcal{R}}(k)^2, \; B_k^{\rm ortho} \approx B_k^{\rm equil} + 2 B_k^{\rm folded}, \; B_{k_S, k_L}^{\rm loc} \approx \frac{12}{5} f_{\rm NL}^{\rm loc} \left[P_{\mathcal{R}}(k_S) P_{\mathcal{R}}(k_L) \right]. \tag{2.66}$$

In the local squeezed limit it is customary to introduce $k_{\rm S}$ for the short wavelength mode and $k_{\rm L}$ for the long wavelength mode.

We have summarized the experimentally determined values for the parameters introduced above in Table 2.1.

Scalar Power Spectrum	Scalar Bispectrum	Tensor Power Spectrum
$\ln(10^{10} A_s) = 3.094 \pm 0.034 \; (1\sigma)$	$f_{\rm NL}^{\rm loc} = 0.8 \pm 5 \; (1\sigma)$	$r < 0.09 \; (2\sigma)$
$n_s = 0.9645 \pm 0.0049 \; (1\sigma)$	$f_{\rm NL}^{\rm equil} = -4 \pm 43 \; (1\sigma)$	$n_t = -r/8$ (assumed)
	$f_{\rm NL}^{\rm ortho} = -26 \pm 21 \; (1\sigma)$	

Table 2.1: Cosmological parameters as measured by Planck TT+TE+EE+lowP [1, 3, 4, 5]. The pivot scale used by the Planck experiment is $k_* = 0.05$ Mpc^{-1}. The tensor-to-scalar ratio is combined with data from BICEP2/KECK array [6]. The assumed form of the tensor tilt n_t follows from the predictions of single field slow-roll inflation with Bunch-Davies mode functions. Future generations of experiments will be able to significantly improve the precision of these measurements [12, 29, 54, 73].

Given the Bunch-Davies solutions previously introduced we may compute analytical expressions for the cosmological parameters. The predictions for the Bunch-Davies mode functions are

$$A_S = \frac{1}{8\pi^2 \epsilon} \frac{H^2}{M_P^2}, \quad n_s = 1 + 2\eta - 4\epsilon, \quad \eta = \frac{\ddot{\phi}}{H |\dot{\phi}|}, \tag{2.67}$$

$$f_{\rm NL}^{\rm loc} \approx \frac{5}{12}(1-n_s), \quad r = 16\epsilon, \quad n_t = -r/8. \tag{2.68}$$

We have not discussed in detail how one computes the primordial scalar bispectrum from the redefined cubic action for $\mathcal{R}$. We will give more details of this computation when we compute the $f_{\rm NL}^{\rm loc}$ parameter for the case of a non-Bunch-Davies solution later in this study. We will only use the local limit $f_{\rm NL}$ parameter since it is the most precisely measured template. In particular, we will describe how the observational limit on $f_{\rm NL}^{\rm loc}$ translates into a bound on the excitation amplitude for excited initial states.

Chapter 3

Excited initial states

Primordial observables depend both which degrees of freedom in the correlation function and the state which those operators are in. Typically, predictions for primordial observables are given assuming that the operators occupy the state of lowest energy density. For the scalar fluctuations this state is termed the Bunch-Davies state [67]. A similar statement holds for tensor fluctuations.

We will begin by reviewing some properties and notation associated with Bogoliubov transformations in section 3.1. We will present how excited states modify the parameters characterizing the scalar power spectrum and the tensor power spectrum in section 3.2. The scalar bispectrum will be computed for excited states in section 3.3. A summary of how observables are changed by the presence of excited states is presented in section 3.4. We bound the amplitude of scalar fluctuation excitations in section 3.5.[1]

[1]Some of the results in this chapter are based on [13, 14, 15].

3.1 Bogoliubov transformations

We will consider states with non-zero occupation number which are termed Bogoliubov excited states. There is no reason a priori to assume that the occupation number for the scalar and tensor perturbations are zero in the early universe. We express both the mode functions and the creation/annihilation operators as a Bogoliubov transformation such that the position space field operator is left unchanged. Explicitly we may write [67]

$$\hat{\mathcal{R}}(\vec{x}) = \int \frac{d^3k}{(2\pi)^3}\, \hat{\mathcal{R}}_{\vec{k}}\, e^{i\vec{k}\cdot\vec{x}} \text{ with } \hat{\mathcal{R}}_{\vec{k},\text{excited}} = \hat{\mathcal{R}}_{\vec{k},\text{BD}}. \tag{3.1}$$

We have introduced

$$\hat{\mathcal{R}}_{\vec{k},\text{excited}} = \mathcal{R}_{k,\text{excited}}\, \hat{a}^{\dagger}_{\vec{k},\text{excited}} + \mathcal{R}^{*}_{k,\text{excited}}\, \hat{a}_{-\vec{k},\text{excited}}, \tag{3.2}$$

and

$$\hat{\mathcal{R}}_{\vec{k},\text{BD}} = \mathcal{R}_{k,\text{BD}}\, \hat{a}^{\dagger}_{\vec{k},\text{BD}} + \mathcal{R}^{*}_{k,\text{BD}}\, \hat{a}_{-\vec{k},\text{BD}}. \tag{3.3}$$

A similar expression holds for the tensor fluctuations.

By making the ansatz that the excited mode functions are a linear combination of the Bunch-Davies mode functions, we may use the condition that $\hat{\mathcal{R}}_{\vec{k},\text{excited}} = \hat{\mathcal{R}}_{\vec{k},\text{BD}}$ to express both the mode functions and the creation/annihilation operators as

$$\mathcal{R}_{k,\text{excited}} = \alpha_k\, \mathcal{R}_{k,\text{BD}} + \beta_k\, \mathcal{R}^{*}_{k,\text{BD}}, \quad \hat{a}^{\dagger}_{\vec{k},\text{excited}} = \alpha^{*}_k\, \hat{a}^{\dagger}_{\vec{k},\text{BD}} - \beta^{*}_k\, \hat{a}_{-\vec{k},\text{BD}}, \tag{3.4}$$

and

$$h^{s}_{k,\text{excited}} = \tilde{\alpha}^{s}_k\, h^{s}_{k,\text{BD}} + \tilde{\beta}^{s}_k\, h^{s*}_{k,\text{BD}}, \quad \hat{b}^{s\dagger}_{\vec{k},\text{excited}} = \tilde{\alpha}^{s}_k\, \hat{b}^{s}_{\vec{k},\text{BD}} - \tilde{\beta}^{s}_k\, \hat{b}^{s\dagger}_{-\vec{k},\text{BD}}. \tag{3.5}$$

It may be easily shown that $\hat{\mathcal{R}}_{\vec{k},\text{excited}} = \hat{\mathcal{R}}_{\vec{k},\text{BD}}$ if and only if $|\alpha_k|^2 - |\beta_k|^2 = 1$. Explicitly,

$$\begin{pmatrix} \mathcal{R}_{k,\text{excited}}\, \hat{a}^\dagger_{\vec{k},\text{excited}} \\ +\mathcal{R}^*_{k,\text{excited}}\, \hat{a}_{-\vec{k},\text{excited}} \end{pmatrix} = \begin{pmatrix} \left(\alpha_k\, \mathcal{R}_{k,\text{BD}} + \beta_k\, \mathcal{R}^*_{k,\text{BD}}\right)\left(\alpha^*_k\, \hat{a}^\dagger_{\vec{k},\text{BD}} - \beta^*_k\, \hat{a}_{-\vec{k},\text{BD}}\right) \\ +\left(\alpha^*_k\, \mathcal{R}^*_{k,\text{BD}} + \beta^*_k\, \mathcal{R}_{k,\text{BD}}\right)\left(\alpha_k\, \hat{a}_{-\vec{k},\text{BD}} - \beta_k\, \hat{a}^\dagger_{\vec{k},\text{BD}}\right) \end{pmatrix} \tag{3.6}$$

Expanding the right hand side yields the desired relation

$$\hat{\mathcal{R}}_{\vec{k},\text{excited}} = \hat{\mathcal{R}}_{\vec{k},\text{BD}}\left(|\alpha_k|^2 - |\beta_k|^2\right) = \hat{\mathcal{R}}_{\vec{k},\text{BD}}. \tag{3.7}$$

For the case of the tensor fluctuations the appropriate condition is that $|\tilde{\alpha}^s_k|^2 - |\tilde{\beta}^s_k|^2 = 1$.

Satisfying the canonical commutation relation in the unexcited vacuum requires that $|\alpha_k|^2 - |\beta_k|^2 = 1$. The canonical commutation relation is given by

$${}_{\text{BD}}\langle 0|\left[\hat{\mathcal{R}}(\vec{x}), \hat{\Pi}_{\mathcal{R}}(\vec{y})\right]|0\rangle_{\text{BD}} = i(2\pi)^3\delta^3\left(\vec{x}-\vec{y}\right) \text{ with } \Pi_{\mathcal{R}} = \frac{\partial \mathcal{L}}{\partial \dot{\mathcal{R}}} = 2a^3\, M_P^2\, \epsilon\, \dot{\mathcal{R}}. \tag{3.8}$$

We may Fourier expand both $\mathcal{R}$ and $\dot{\mathcal{R}}$ allowing us to reduce the commutator to a commutator of creation and annihilation operators. We have previously done this for the unexcited operator, showing that the mode function $\mathcal{R}_{k,\text{BD}}$ satisfies the canonical commutation condition. Using (3.7) we may easily verify that the excited mode functions will satisfy the canonical commutation relation as well as long as $|\alpha_k|^2 - |\beta_k|^2 = 1$. Explicitly,

$$\begin{gathered} 2a^3 M_P^2 \epsilon \int \frac{d^3k}{(2\pi)^3} \int \frac{d^3p}{(2\pi)^3} e^{i\vec{k}\cdot\vec{x}} e^{i\vec{p}\cdot\vec{y}}\, {}_{\text{BD}}\langle 0|\left[\hat{\mathcal{R}}_{\vec{k},\text{excited}}, \dot{\hat{\mathcal{R}}}_{\vec{p},\text{excited}}\right]|0\rangle_{\text{BD}} \\ = i(2\pi)^3\delta^3\left(\vec{x}-\vec{y}\right) \end{gathered} . \tag{3.9}$$

Using (3.7) we immediately obtain our desired result,

$$2a^3 M_P^2 \epsilon \int \frac{d^3k}{(2\pi)^3} \int \frac{d^3p}{(2\pi)^3} e^{i\vec{k}\cdot\vec{x}} e^{i\vec{p}\cdot\vec{y}} \, {}_{\rm BD}\langle 0| \left[\hat{\mathcal{R}}_{\vec{k},\rm BD}, \dot{\hat{\mathcal{R}}}_{\vec{p},\rm BD}\right] |0\rangle_{\rm BD} \left(|\alpha_k|^2 - |\beta_k|^2\right) = i(2\pi)^3 \delta^3\left(\vec{x} - \vec{y}\right) \tag{3.10}$$

Comparison with (2.53) verifies that we require $|\alpha_k|^2 - |\beta_k|^2 = 1$. A similar argument may be made for the tensor perturbation normalization condition.

The relationship between particle occupation number and the Bogoliubov coefficients may be made explicit by considering the number operator. The occupation number is the expectation value of the excited number operator acting on the unexcited vacuum [10, 22, 67],

$$n_{\vec{k}} = {}_{\rm BD}\langle 0|\hat{N}_{\vec{k},\rm excited}|0\rangle_{\rm BD} = {}_{\rm BD}\langle 0|\hat{a}^\dagger_{\vec{k},\rm excited}\hat{a}_{\vec{k},\rm excited}|0\rangle_{\rm BD}. \tag{3.11}$$

We may expand the excited operators in terms of the unexcited operators (3.4) which may directly act on the unexcited vacuum

$$n_{\vec{k}} = {}_{\rm BD}\langle 0| \left(\alpha_k^* \, \hat{a}^\dagger_{\vec{k},\rm BD} - \beta_k^* \, \hat{a}_{-\vec{k},\rm BD}\right) \left(\alpha_k \, \hat{a}_{\vec{k},\rm BD} - \beta_k \, \hat{a}^\dagger_{-\vec{k},\rm BD}\right) |0\rangle_{\rm BD} = |\beta_k|^2. \tag{3.12}$$

Therefore we see that the Bogoliubov parameter $|\beta_k|^2$ is a measure of the particle occupation number.

3.2 Scalar and tensor power spectrum corrections

We will compute the power spectrum and bispectrum in the presence of excited states in order to see how excited states change the cosmological parameters we discussed in section 2.6. The scalar power spectrum has been

computed for the case of the Bunch-Davies vacuum (2.61). The computation is analogous for the case of non-Bunch-Davies (NBD) vacua that we are considering here. We would like to express the late time power spectrum for excited states in terms of the late time power spectrum for the Bunch-Davies vacuum to see the deviation from the usual prediction. Both the power spectrum amplitude A_s and the spectral index n_s are modified by the presence of excited states.

We will begin by computing the correction to the power spectrum amplitude A_s. The approach will be to study the relationship between the excited mode function and the Bunch-Davies mode function at late time. Explicitly we have

$$_{\rm NBD}\langle 0|\hat{\mathcal{R}}_{\vec{k},\rm excited}\hat{\mathcal{R}}_{\vec{k}_2,\rm excited}|0\rangle_{\rm NBD} = (2\pi)^3\delta^3\left(\vec{k}+\vec{k}_2\right)|\mathcal{R}_{k,\rm excited}|^2. \tag{3.13}$$

We may expand the excited mode function in terms of the Bunch-Davies mode function in the usual way

$$\begin{aligned} |\mathcal{R}_{k,\rm excited}|^2 &= \left(\alpha_k^*\mathcal{R}_{k,\rm BD}^* + \beta_k^*\mathcal{R}_{k,\rm BD}\right)\left(\alpha_k\mathcal{R}_{k,\rm BD} + \beta_k\mathcal{R}_{k,\rm BD}^*\right) \\ &= \left(|\alpha_k|^2 + |\beta_k|^2\right)|\mathcal{R}_{k,\rm BD}|^2 + \alpha_k\beta_k^*\left(\mathcal{R}_{k,\rm BD}\right)^2 + \alpha_k^*\beta_k\left(\mathcal{R}_{k,\rm BD}^*\right)^2. \end{aligned} \tag{3.14}$$

At late times, the terms in the Bunch-Davies mode functions of the form (k/aH) vanish. Therefore at late times $\mathcal{R}_{k,\rm BD,late} = \mathcal{R}_{k,\rm BD,late}^*$ and we may write

$$|\mathcal{R}_{k,\rm excited,late}|^2 = |\mathcal{R}_{k,\rm BD,late}|^2|\alpha_{k_*} + \beta_{k_*}|^2. \tag{3.15}$$

This implies that we may express the change in power spectrum amplitude by

a multiplicative factor which is positive definite,

$$A_{s,\text{excited}} = A_{s,\text{BD}}\,|\alpha_{k_*} + \beta_{k_*}|^2. \tag{3.16}$$

We remind the reader that k_* corresponds to the pivot scale as was discussed in section 2.6.

The change in the scalar spectral index n_s due to the presence of excited states will turn out to be an additive correction as opposed to a multiplicative correction. Explicitly we have

$$n_{s,\text{excited}} - 1 = \frac{d\ln\Delta^2_{\mathcal{R},\text{excited}}}{d\ln k} = \frac{d\ln\Delta^2_{\mathcal{R},\text{BD}}}{d\ln k} + \frac{d\ln|\alpha_k + \beta_k|^2}{d\ln k}. \tag{3.17}$$

We will bound $|\alpha_k + \beta_k|$ using these expressions for A_s and n_s in section 3.5.

Similar arguments to those made for the scalar power spectrum apply to the tensor power spectrum. The correction to the amplitude is given by

$$(r_{\text{excited}}\,A_{s,\text{excited}}) = (r_{\text{BD}}\,A_{s,\text{BD}})\,|\tilde{\alpha}_{k_*} + \tilde{\beta}_{k_*}|^2. \tag{3.18}$$

In principle the two helicities need not be excited by the same amount. There are examples where this is the case [18, 35, 38, 37, 68, 69, 85]. However, we will assume that $\tilde{\alpha}^s_k \approx \tilde{\alpha}_k$ and $\tilde{\beta}^s_k \approx \tilde{\beta}_k$ as was done in [14]. It is immediately clear that the correction to the tensor-to-scalar ratio is simply given by [14]

$$r_{\text{excited}} = r_{\text{BD}}\frac{|\tilde{\alpha}_{k_*} + \tilde{\beta}_{k_*}|^2}{|\alpha_{k_*} + \beta_{k_*}|^2}. \tag{3.19}$$

The tensor spectral tilt is corrected by [16, 17]

$$n_{t,\text{excited}} = \frac{d\ln\Delta^2_{t,\text{excited}}}{d\ln k} = \frac{d\ln\Delta^2_{t,\text{BD}}}{d\ln k} + \frac{d\ln|\tilde{\alpha}_k + \tilde{\beta}_k|^2}{d\ln k}. \tag{3.20}$$

Since we have not observed primordial tensor excitations directly nor indirectly, it is difficult to constrain the parameters $\tilde{\alpha}_k$ and $\tilde{\beta}_k$. We will primarily be interested in scalar observables since there are physical mechanisms which easily excite scalar fluctuations while leaving tensor fluctuations unexcited as we have discussed in section 2.4. However, if the primordial tensor spectrum is eventually observed the corrections to these quantities may play a role.

3.3 Scalar bispectrum corrections

In this section we will compute the scalar bispectrum and present the corrections to the $f_{\rm NL}^{\rm loc}$ parameter due to the presence of excited initial states. Historically, non-gaussianity was thought to be a suitable way to probe for the existence of excited initial states [9, 26, 42, 45, 51, 65]. However, bounds from scale invariance and backreaction considerations have subsequently shown that the enhancement to the local squeezed limit $f_{\rm NL}^{\rm loc}$ is not substantial [13, 40, 47] for the usual single field model which we have discussed thus far. We will present the bound on the excitation amplitude which arises from the observational bound on $f_{\rm NL}^{\rm loc}$ in section 3.5.

3.3.1 Motivation and setup

As discussed earlier in section 2.4, the cubic action for $\mathcal{R}$ is unwieldy and makes the computation of the three point function of $\mathcal{R}$ difficult. It is advantageous to instead use a redefined variable $\mathcal{R}_c$ as first emphasized by [63]. The difference between the three point function of $\mathcal{R}$ and the three

point function of $\mathcal{R}_c$ takes the form of a product of two point functions of $\mathcal{R}$. Therefore we trade the computationally hard problem of $\langle \mathcal{R}^3 \rangle$ for the computationally easy problem of $\langle \mathcal{R}_c^3 \rangle$ and $\langle \mathcal{R}^2 \rangle$.

The three point function we would like to compute is schematically given by [63]

$$\begin{aligned} \langle \hat{\mathcal{R}}\hat{\mathcal{R}}\hat{\mathcal{R}} \rangle = \; & \langle \hat{\mathcal{R}}_c\hat{\mathcal{R}}_c\hat{\mathcal{R}}_c \rangle \\ & + \lambda \left(\langle \hat{\mathcal{R}}(x_1)\hat{\mathcal{R}}(x_2) \rangle \langle \hat{\mathcal{R}}(x_1)\hat{\mathcal{R}}(x_3) \rangle + (x_2 \leftrightarrow x_3) + \text{cyclic} \right). \end{aligned} \tag{3.21}$$

We will proceed by computing each piece individually in sections 3.3.2 and 3.3.3. The total three point function will be presented in section 3.3.4 in order to discuss observable templates in section 3.3.5.

3.3.2 Shifted three point function

The third order action for the shifted scalar fluctuations is given by (2.43),

$$S_{3,c} = 4\epsilon^2 H M_P^2 \int d^4x \, a^5 \, \dot{\mathcal{R}}_c^2 \left(\partial^{-2} \dot{\mathcal{R}}_c \right) = 4\epsilon^2 H M_P^2 \int d^3x \, d\tau \, a^3 \mathcal{R}_c'^2 \left(\partial^{-2} \mathcal{R}_c' \right). \tag{3.22}$$

From a Legendre transformation of the relevant interaction Lagrangian we obtain the relevant interaction Hamiltonian. There are two non-vanishing leading order contributions to the shifted scalar fluctuation three point function. There is the contribution arising from expanding the unitary operator on the left and the contribution from expanding the unitary operator on the

right. Schematically we may write

$$\langle 0|e^{\left[i\int_{-\infty}^{t} dt_1\ H(t_1)\right]}\hat{\mathcal{R}}_c\hat{\mathcal{R}}_c\hat{\mathcal{R}}_c e^{\left[-i\int_{-\infty}^{t} dt_1\ H(t_1)\right]}|0\rangle \approx 2\mathrm{Re}\left[\text{right insertion result}\right]. \tag{3.23}$$

The first step of the computation is to Fourier expand the relevant field operators. For compactness, we will drop the "excited" subscript during this calculation. In particular,

$$\langle\hat{\mathcal{R}}_c(x_1)\hat{\mathcal{R}}_c(x_2)\hat{\mathcal{R}}_c(x_3)\rangle = \prod_{n=1}^{3}\left[\int\frac{d^3k_i}{(2\pi)^3}e^{i\vec{k}_i\cdot\vec{x}_i}\right]\langle\hat{\mathcal{R}}_{\vec{k}_1,c}\hat{\mathcal{R}}_{\vec{k}_2,c}\hat{\mathcal{R}}_{\vec{k}_3,c}\rangle. \tag{3.24}$$

Expanding the exponential on the right in (3.23) allows us to compute the momentum space three point function. We obtain the following expression

$$\langle\hat{\mathcal{R}}_{\vec{k}_1,c}\hat{\mathcal{R}}_{\vec{k}_2,c}\hat{\mathcal{R}}_{\vec{k}_3,c}\rangle = 2\times 2\mathrm{Re}\left\{\left(i4\epsilon^2HM_P^2\right)C_{\mathrm{ext}}\times(2\pi)^3\delta^3\left(\vec{k}_1+\vec{k}_2+\vec{k}_3\right)C_{\mathrm{int}}\right\}, \tag{3.25}$$

This simplified form is obtained after rewriting the propagators in terms of the mode functions as follows

$$\langle\mathcal{R}_{\vec{k}}(\tau)\widetilde{\mathcal{R}}(\vec{w},\tau_2)\rangle = \int\frac{d^3p}{(2\pi)^3}\langle 0|\hat{\mathcal{R}}_{\vec{k}}\hat{\widetilde{\mathcal{R}}}_{\vec{p}}|0\rangle e^{i\vec{p}\cdot\vec{w}} = \mathcal{R}^*_{k,\tau}\widetilde{\mathcal{R}}_{k,\tau_2}e^{-i\vec{k}\cdot\vec{w}}. \tag{3.26}$$

The internal spatial coordinate integral gave rise to the momentum conserving delta function. The parameter C_{ext} contains the internal time integral as well as the external field operator mode functions

$$C_{\mathrm{ext}} = \int d\tau_2\left(-\frac{1}{\tau_2 H}\right)^3\prod_{n=1}^{3}\left[\mathcal{R}^*_{k_n,\tau}\right]. \tag{3.27}$$

The parameter C_{int} contains the internal mode functions

$$C_{\mathrm{int}} = \left[\sum_{m=1}^{3}\left(\frac{1}{(ik_m)^2}\right)\mathcal{R}'_{k_1,\tau_2}\mathcal{R}'_{k_2,\tau_2}\mathcal{R}'_{k_3,\tau_2}\right]. \tag{3.28}$$

We will explicitly expand the mode functions in terms of the Bogoliubov parameters so that we may perform the τ_2 integral. The mode function terms expand as

$$C_{\rm ext} = \left(\frac{1}{\sqrt{2\epsilon}}\frac{H}{M_P\sqrt{2}}\right)^3 \prod_{n=1}^{3}\left[\left(\frac{1}{k_n}\right)^{3/2}\left(\alpha^*_{k_n}+\beta^*_{k_n}\right)\right]\int d\tau_2\left(-\frac{1}{\tau_2 H}\right)^3, \quad (3.29)$$

and

$$C_{\rm int} = \left(\frac{1}{\sqrt{2\epsilon}}\frac{H}{M_P\sqrt{2}}\right)^3 \tau_2^3\left[\sum_{m=1}^{3}\left(\frac{1}{(ik_m)^2}\right)\prod_{q=1}^{3}k_q^{1/2}\left(\alpha_{k_q}e^{ik_q\tau_2}+\beta_{k_q}e^{-ik_q\tau_2}\right)\right]. \quad (3.30)$$

The external leg mode functions are evaluated at late time since we eventually take $k\tau \to 0$ at the end of the calculation. The internal mode functions are integrated from $\tau_2 \to -\infty$ to $\tau_2 \to \tau$, so there is no such simplification.

We may perform the τ_2 integral yielding a relatively simple expression

$$\begin{aligned}\langle\hat{\mathcal{R}}_{\vec{k}_1,c}\hat{\mathcal{R}}_{\vec{k}_2,c}\hat{\mathcal{R}}_{\vec{k}_3,c}\rangle = \frac{2}{\epsilon}\frac{H^4}{M_P^4}{\rm Re}\left\{\prod_{n=1}^{3}\left[\left(\frac{1}{2k_n^3}\right)\left(\alpha^*_{k_n}+\beta^*_{k_n}\right)\right]\right.\\ \times\frac{1}{2}\sum_{m=1,j\neq m}^{3}\left(k_m^2k_j^2\right)(2\pi)^3\delta^3\left(\vec{k}_1+\vec{k}_2+\vec{k}_3\right)\\ \left.\times\left[\left(\frac{\alpha_{k_1}\alpha_{k_2}\alpha_{k_3}-\beta_{k_1}\beta_{k_2}\beta_{k_3}}{k_1+k_2+k_3}\right)+\left(\frac{\alpha_{k_1}\alpha_{k_2}\beta_{k_3}-\beta_{k_1}\beta_{k_2}\alpha_{k_3}}{k_1+k_2-k_3}+{\rm cyclic}\right)\right]\right\}\end{aligned} \quad (3.31)$$

3.3.3 Redefinition terms

We have shifted $\mathcal{R}$ to simplify the cubic action as [63]

$$\begin{aligned}\mathcal{R} &= \mathcal{R}_c + \frac{1}{2}\frac{\ddot{\phi}}{\dot{\phi}H}\mathcal{R}_c^2 + \frac{1}{8}\frac{\dot{\phi}^2}{H^2M_P^2}\mathcal{R}_c^2 + \frac{1}{4}\frac{\dot{\phi}^2}{H^2M_P^2}\partial^{-2}\left(\mathcal{R}_c\partial^2\mathcal{R}_c\right)+\cdots\\ &= \mathcal{R}_c - \frac{1}{2}\eta\mathcal{R}_c^2 + \frac{1}{4}\epsilon\mathcal{R}_c^2 + \frac{1}{2}\epsilon\partial^{-2}\left(\mathcal{R}_c\partial^2\mathcal{R}_c\right)+\cdots.\end{aligned} \quad (3.32)$$

This schematically results in a shift of the form $\mathcal{R} = \mathcal{R}_c + \lambda \mathcal{R}_c^2 + \cdots$. We may explicitly Fourier expand the redefinition term, substituting the appropriate expression for λ

$$\begin{aligned}(\text{redef term}) &= \int \frac{d^3k_2}{(2\pi)^3}\frac{d^3k_3}{(2\pi)^3}\left(-\eta + \frac{1}{2}\epsilon + \frac{1}{2}\epsilon\frac{k_2^2+k_3^2}{(\vec{k}_2+\vec{k}_3)^2}\right) \\ &\times \left(|\mathcal{R}_{k_2,\text{BD}}|^2|\mathcal{R}_{k_3,\text{BD}}|^2|\alpha_{k_2}+\beta_{k_2}|^2|\alpha_{k_3}+\beta_{k_3}|^2 e^{i\vec{k}_2\cdot(\vec{x}_1-\vec{x}_2)}e^{i\vec{k}_3\cdot(\vec{x}_1-\vec{x}_3)}\right) + \text{cyclic}\end{aligned} \tag{3.33}$$

We have already expanded the excited state two point function in terms of the Bunch-Davies two point function. Plugging in the late time mode functions allows all factors of momentum to be written explicitly

$$\begin{aligned}(\text{redef term}) &= \frac{1}{(4\times 4)\epsilon^2}\frac{H^4}{M_P^4}\int \frac{d^3k_2}{(2\pi)^3}\frac{d^3k_3}{(2\pi)^3}\left(-\eta + \frac{1}{2}\epsilon + \frac{1}{2}\epsilon\frac{k_2^2+k_3^2}{(\vec{k}_2+\vec{k}_3)^2}\right) \\ &\times \left(\frac{1}{k_2^3\,k_3^3}|\alpha_{k_2}+\beta_{k_2}|^2|\alpha_{k_3}+\beta_{k_3}|^2 e^{i\vec{k}_2\cdot(\vec{x}_1-\vec{x}_2)}e^{i\vec{k}_3\cdot(\vec{x}_1-\vec{x}_3)}\right) + \text{cyclic}\end{aligned} \tag{3.34}$$

To make the expression more compatible with the $\mathcal{R}_c$ three point function we have previously computed, we will reintroduce the momentum k_1 and a delta function

$$\begin{aligned}(\text{redef term}) &= \frac{1}{(4\times 4)\epsilon^2}\frac{H^4}{M_P^4}\prod_{i=1}^{3}\left[\int\frac{d^3k_i}{(2\pi)^3}\right](2\pi)^3\delta^3\left(\vec{k}_1+\vec{k}_2+\vec{k}_3\right) \\ &\times \left(-\eta + \frac{1}{2}\epsilon + \frac{1}{2}\epsilon\frac{k_2^2+k_3^2}{k_1^2}\right)\left(\frac{1}{k_2^3\,k_3^3}|\alpha_{k_2}+\beta_{k_2}|^2|\alpha_{k_3}+\beta_{k_3}|^2 e^{i\vec{k}_2\cdot(\vec{x}_1-\vec{x}_2)}e^{i\vec{k}_3\cdot(\vec{x}_1-\vec{x}_3)}\right) \\ &+\text{cyclic}\end{aligned} \tag{3.35}$$

We may express this in a more convenient form which enables us to combine it with the three point function of $\mathcal{R}_c$ more easily,

$$\begin{aligned}(\text{redef term}) = \quad & \frac{1}{2\epsilon^2}\frac{H^4}{M_P^4}\prod_{n=1}^{3}\left[\int \frac{d^3k_n}{(2\pi)^3}\frac{|\alpha_{k_n}+\beta_{k_n}|^2}{2k_n^3}e^{-i\vec{k}_n\cdot\vec{x}_n}\right](2\pi)^3\delta^3\left(\vec{k}_1+\vec{k}_2+\vec{k}_3\right) \\ & \times\sum_{m=1}^{3}\left(-\eta\frac{k_m^3}{|\alpha_{k_m}+\beta_{k_m}|^2}+\frac{1}{2}\epsilon\frac{k_m^3}{|\alpha_{k_m}+\beta_{k_m}|^2}+\frac{1}{2}\epsilon\sum_{j\neq m}k_m k_j^2\right)\end{aligned} . \tag{3.36}$$

3.3.4 Three point function

Having computed the shifted three point function and the term arising from the redefinition of $\mathcal{R}$, we may now add them together to obtain the three point function for the original comoving curvature perturbation $\mathcal{R}$

$$\langle\hat{\mathcal{R}}(\vec{x}_1)\hat{\mathcal{R}}(\vec{x}_2)\hat{\mathcal{R}}(\vec{x}_3)\rangle = \prod_{m=1}^{3}\left[\int\frac{d^3k_m}{(2\pi)^3}e^{-i\vec{k}_m\cdot\vec{x}_m}\right]\langle\hat{\mathcal{R}}_{\vec{k}_1}\hat{\mathcal{R}}_{\vec{k}_2}\hat{\mathcal{R}}_{\vec{k}_3}\rangle. \tag{3.37}$$

The functional form of the momentum space three point function is

$$\langle\hat{\mathcal{R}}_{\vec{k}_1}\hat{\mathcal{R}}_{\vec{k}_2}\hat{\mathcal{R}}_{\vec{k}_3}\rangle = \frac{H^4}{2\epsilon^2 M_P^4}\left[\prod_{n=1}^{3}\frac{1}{2k_n^3}\right](2\pi)^3\delta^3\left(\vec{k}_1+\vec{k}_2+\vec{k}_3\right)A_{k_1,k_2,k_3} \tag{3.38}$$

We have let

$$\begin{aligned}A_{k_1,k_2,k_3} \quad = \quad & 2\epsilon\left(\sum_{m=1,j\neq m}^{3}k_m^2k_j^2\right)\left[\prod_{n=1}^{3}\left(\alpha_{k_n}^*+\beta_{k_n}^*\right)\right]\text{Re}\left[M_{k_1,k_2,k_3}\right] \\ & +\left(\prod_{n=1}^{3}|\alpha_{k_n}+\beta_{k_n}|^2\right)N_{k_1,k_2,k_3}\end{aligned} . \tag{3.39}$$

Where we have defined

$$M_{k_1,k_2,k_3} = \left(\frac{\alpha_{k_1}\alpha_{k_2}\alpha_{k_3}-\beta_{k_1}\beta_{k_2}\beta_{k_3}}{k_1+k_2+k_3}\right)+\left(\frac{\alpha_{k_1}\alpha_{k_2}\beta_{k_3}-\beta_{k_1}\beta_{k_2}\alpha_{k_3}}{k_1+k_2-k_3}+\text{cyclic}\right), \tag{3.40}$$

and

$$N_{k_1,k_2,k_3} = \sum_{m=1}^{3} \left(-\eta \frac{k_m^3}{|\alpha_{k_m} + \beta_{k_m}|^2} + \frac{1}{2}\epsilon \frac{k_m^3}{|\alpha_{k_m} + \beta_{k_m}|^2} + \frac{1}{2}\epsilon \sum_{j \neq m} \frac{k_m k_j^2}{|\alpha_{k_m} + \beta_{k_m}|^2} \right). \tag{3.41}$$

For the case of the Bunch-Davies state this result simplifies to

$$A^{\mathrm{BD}}_{k_1,k_2,k_3} = \frac{2\epsilon}{k_1 + k_2 + k_3} \left(\sum_{m=1, j \neq m}^{3} k_m^2 k_j^2 \right) + \sum_{m=1}^{3} \left(-\eta k_m^3 + \frac{1}{2}\epsilon k_m^3 + \frac{1}{2}\epsilon \sum_{j \neq m} k_m k_j^2 \right). \tag{3.42}$$

We have presented the solution for the three point function of the comoving curvature perturbation in the presence of excited states. Usually specific configurations of momentum are considered which allow us to discuss an amplitude of the three-point function. In the next section we will revisit the connection between the bispectrum and the f_{NL} parameter first introduced in section 2.6.

3.3.5 Bispectrum templates

The bispectrum is closely related to the momentum space three point function in the following way

$$\langle \hat{\mathcal{R}}_{\vec{k}_1} \hat{\mathcal{R}}_{\vec{k}_2} \hat{\mathcal{R}}_{\vec{k}_3} \rangle = (2\pi)^3 \delta^3 \left(\vec{k}_1 + \vec{k}_2 + \vec{k}_3 \right) B_{k_1,k_2,k_3}. \tag{3.43}$$

Having computed the momentum space three point function (3.38), we may write the bispectrum explicitly as

$$B_{k_1,k_2,k_3} = \frac{H^4}{2\epsilon^2 M_P^4} \left[\prod_{m=1}^{3} \frac{1}{2k_m^3} \right] A_{k_1,k_2,k_3}. \tag{3.44}$$

There is a momentum independent amplitude associated with the three point function which is referred to as f_{NL}. Specifically,

$$B_{k_1,k_2,k_3} = \frac{6}{5} f_{\rm NL} \left[P_{\mathcal{R}}(k_1) P_{\mathcal{R}}(k_2) + P_{\mathcal{R}}(k_2) P_{\mathcal{R}}(k_3) + P_{\mathcal{R}}(k_3) P_{\mathcal{R}}(k_1) \right]. \quad (3.45)$$

Observational bounds on non-gaussianity are reported as bounds on the size of $f_{\rm NL}$ for a given configuration of momentum [4].

Different momenta configurations correspond to different shape limits which are reported from experimental searches. The three templates which are commonly used [19] are the local squeezed limit ($k_1 \approx k_2 \gg k_3$), the equilateral limit ($k_1 \approx k_2 \approx k_3$) and the folded limit ($k_1 \approx k_2 \approx k_3/2$). Instead of the folded limit, a linear combination of the folded limit and the equilateral limit is typically used [4]. This template is referred to as the orthogonal template [76]. We will compute $f_{\rm NL}^{\rm loc}$ since it is the most precisely measured of the three commonly used templates.

3.3.5.1 Local squeezed limit

The local squeezed limit ($k_1 \approx k_2 \approx k \gg k_3$) bispectrum has dominant contributions from terms which include the small momentum k_3 in the denominator. It is customary to refer to the short wavelength mode as $k_{\rm S}$ and the long wavelength mode as $k_{\rm L}$. In terms of $f_{\rm NL}$ we simply have

$$B^{\rm loc}_{k_{\rm S},k_{\rm L}} \approx \frac{12}{5} f^{\rm loc}_{\rm NL} \left[P_{\mathcal{R}}(k_{\rm S}) P_{\mathcal{R}}(k_{\rm L}) \right]. \quad (3.46)$$

We begin by computing the squeezed limit non-gaussianity for the case of the Bunch-Davies state which was already presented in (2.68). The form of

$A^{\rm loc}_{k_{\rm S},k_{\rm L}}$ may be obtained directly by substituting the momenta limits in

$$A^{\rm loc,BD}_{k_{\rm S},k_{\rm L}} \approx \frac{2\epsilon}{2k_{\rm S}}(2k_{\rm S}^4) + k_{\rm S}^3\left(-2\eta+\epsilon+\epsilon\right) = k_{\rm S}^3(-2\eta+4\epsilon) \tag{3.47}$$

This may be written in terms of the scalar spectral index by recalling that $(n_s-1)=(2\eta-4\epsilon)$. The resulting simple form of $A^{\rm loc}_{k_{\rm S},k_{\rm L}}$ is

$$A^{\rm loc,BD}_{k_{\rm S},k_{\rm L}} \approx k_{\rm S}^3(1-n_s). \tag{3.48}$$

The squeezed limit bispectrum becomes

$$B^{\rm loc,BD}_{k_{\rm S},k_{\rm L}} \approx \frac{H^4}{16\epsilon^2 M_P^4}\frac{1}{k_{\rm S}^3 k_{\rm L}^3}(1-n_s). \tag{3.49}$$

The power spectra product that enters into formula (3.46) relating the bispectrum and $f_{\rm NL}$ is given by

$$P_{\mathcal{R}}(k_{\rm S})P_{\mathcal{R}}(k_{\rm L}) = \frac{1}{k_{\rm S}^3\,k_{\rm L}^3}\left(\frac{1}{4\epsilon}\frac{H^2}{M_P^2}\right)^2. \tag{3.50}$$

Therefore the squeezed limit $f^{\rm loc}_{\rm NL}$ for the Bunch-Davies state is verified to be the expression given in section 2.6

$$f^{\rm loc,BD}_{\rm NL} \approx \frac{5}{12}\frac{B^{\rm loc,BD}_{k_{\rm S},k_{\rm L}}}{P_{\mathcal{R}}(k_{\rm S})P_{\mathcal{R}}(k_{\rm L})} = \frac{5}{12}(1-n_s). \tag{3.51}$$

We will now compute the expression for the local squeezed limit $f_{\rm NL}$ for the case of excited states to see how it compares to the expression we computed for the Bunch-Davies case. The dominant contributions to $M^{\rm loc}_{k_{\rm S},k_{\rm L}}$ and $N^{\rm loc}_{k_{\rm S},k_{\rm L}}$ for the excited state case are

$$M^{\rm loc}_{k_{\rm S},k_{\rm L}} \approx 2\frac{\alpha_{k_{\rm S}}\beta_{k_{\rm S}}(\alpha_{k_{\rm L}}-\beta_{k_{\rm L}})}{k_{\rm L}} \text{ and } N^{\rm loc}_{k_{\rm S},k_{\rm L}} \approx (-2\eta+\epsilon)\,\frac{k_{\rm S}^3}{|\alpha_{k_{\rm S}}+\beta_{k_{\rm S}}|^2}+2\epsilon\frac{k_{\rm S}^3}{|\alpha_{k_{\rm S}}+\beta_{k_{\rm S}}|^2}. \tag{3.52}$$

The term in $A^{\rm loc}_{k_{\rm S},k_{\rm L}}$ proportional to $M^{\rm loc}_{k_{\rm S},k_{\rm L}}$ will be the dominant term due to the presence of $k_{\rm L}$ in the denominator. Therefore $A^{\rm loc}_{k_{\rm S},k_{\rm L}}$ takes the relatively simple form

$$A^{\rm loc}_{k_{\rm S},k_{\rm L}} \approx 8\epsilon \frac{k_{\rm S}^4}{k_{\rm L}} (\alpha^*_{k_{\rm S}} + \beta^*_{k_{\rm S}})^2 (\alpha^*_{k_{\rm L}} + \beta^*_{k_{\rm L}}) {\rm Re}\left[\alpha_{k_{\rm S}} \beta_{k_{\rm S}} \left(\alpha_{k_{\rm L}} - \beta_{k_{\rm L}}\right)\right]. \tag{3.53}$$

We may substitute the expression for $A^{\rm sq}_{k,k_3}$ into the bispectrum formula in order to obtain an explicit expression for the squeezed limit bispectrum

$$B^{\rm loc}_{k_{\rm S},k_{\rm L}} \approx \frac{H^4}{2\epsilon M_P^4} \frac{1}{k_{\rm S}^2 k_{\rm L}^4} (\alpha^*_{k_{\rm S}} + \beta^*_{k_{\rm S}})^2 (\alpha^*_{k_{\rm L}} + \beta^*_{k_{\rm L}}) {\rm Re}\left[\alpha_{k_{\rm S}} \beta_{k_{\rm S}} \left(\alpha_{k_{\rm L}} - \beta_{k_{\rm L}}\right)\right]. \tag{3.54}$$

The power spectrum product that the bispectrum must be divided by now has additional multiplicative factors since the power spectra themselves correspond to excited states

$$P_{\mathcal{R}}(k_{\rm S}) P_{\mathcal{R}}(k_{\rm L}) = \frac{|\alpha_{k_{\rm S}} + \beta_{k_{\rm S}}|^2 |\alpha_{k_{\rm L}} + \beta_{k_{\rm L}}|^2}{k_{\rm S}^3\, k_{\rm L}^3} \left(\frac{1}{4\epsilon} \frac{H^2}{M_P^2}\right)^2. \tag{3.55}$$

The value of $f^{\rm sq}_{\rm NL}$ is determined by dividing the bispectrum by the product of power spectra

$$f^{\rm loc}_{\rm NL} = \frac{5}{12} \frac{B^{\rm loc}_{k_{\rm S},k_{\rm L}}}{P_{\mathcal{R}}(k_{\rm S}) P_{\mathcal{R}}(k_{\rm L})} = \frac{10}{3} \epsilon \left(\frac{k_{\rm S}}{k_{\rm L}}\right) \frac{(\alpha^*_{k_{\rm S}} + \beta^*_{k_{\rm S}})}{(\alpha_{k_{\rm S}} + \beta_{k_{\rm S}})(\alpha_{k_{\rm L}} + \beta_{k_{\rm L}})} {\rm Re}\left[\alpha_{k_{\rm S}} \beta_{k_{\rm S}} \left(\alpha_{k_{\rm L}} - \beta_{k_{\rm L}}\right)\right]. \tag{3.56}$$

This result may be made more illuminating by considering the limit of small $|\beta_k|$. In this case $\alpha_k \approx 1$ since the normalization condition requires that $|\alpha_k| = \sqrt{1 - |\beta_k|^2}$. The simplified expression for the case of small $|\beta_k|$ is proportional to β_k and given by

$$f^{\rm loc}_{\rm NL} \approx \frac{10}{3} \epsilon \left(\frac{k_{\rm S}}{k_{\rm L}}\right) {\rm Re}\left[\beta_{k_{\rm S}}\right]. \tag{3.57}$$

3.4 Summary of corrections

We have shown how the presence of excited initial states modify the cosmological parameters introduced in section 2.6. In summary we have found

$$A_s = A_{s,BD}|\alpha_{k_*} + \beta_{k_*}|^2, \quad n_s = n_{s,BD} + \frac{d\ln|\alpha_k + \beta_k|^2}{d\ln k}, \tag{3.58}$$

$$r = r_{BD}\frac{|\tilde{\alpha}_{k_*} + \tilde{\beta}_{k_*}|^2}{|\alpha_{k_*} + \beta_{k_*}|^2}, \quad n_t = n_{t,BD} + \frac{d\ln|\tilde{\alpha}_k + \tilde{\beta}_k|^2}{d\ln k}, \tag{3.59}$$

$$f_{\rm NL}^{\rm loc} \approx \frac{10}{3}\epsilon\left(\frac{k_{\rm S}}{k_{\rm L}}\right)\frac{(\alpha^*_{k_{\rm S}} + \beta^*_{k_{\rm S}})}{(\alpha_{k_{\rm S}} + \beta_{k_{\rm S}})(\alpha_{k_{\rm L}} + \beta_{k_{\rm L}})}{\rm Re}\left[\alpha_{k_{\rm S}}\beta_{k_{\rm S}}\left(\alpha_{k_{\rm L}} - \beta_{k_{\rm L}}\right)\right]. \tag{3.60}$$

In the next section, we will discuss how observational consistency with the values reported in Table 2.1 allows us to bound the amplitude of excitation.

3.5 Bounds on excitation amplitude

We present the bounds arising from backreaction considerations for different functional forms of Bogoliubov excitations and show that the limits are similar. While previous studies have applied the backreaction bound for a nearly scale invariant spectrum of excitations [13, 14, 40], we revisit this computation and extend it to other functional forms of excitations. Bounds that arise from the measurement of n_s and the observational limits on $f_{\rm NL}^{\rm loc}$ turn out to be weaker than the bounds that are obtained from backreaction considerations.

In section 3.5.1 we will present the bounds that arise from backreaction considerations. In section 3.5.2 we will present the bounds that arise from the measurement of n_s. In section 3.5.3 we present the bounds that arise from the observational limits on $f_{\rm NL}^{\rm loc}$. In section 3.5.4, we will address the special case that only $l \lesssim 30$ modes are excited.

3.5.1 Bounds from backreaction considerations

The scalar power spectrum has been measured to deviate only slightly from scale invariance. This implies that the modes comprising the observable cosmic microwave background should not vary dramatically in amplitude across the approximately 3-4 decades of modes we observe today. Therefore the modes we observe today should either be excited modes or Bunch-Davies modes. We will compute the bounds on excitation parameters implied by this.

In order for all of the modes comprising the CMB to have exited the horizon during inflation, the highest-l mode must be at least $n \approx 3-4$ [52, 53, 71] decades shorter wavelength than the horizon size at the beginning of inflation. To obtain the most conservative bound from backreaction considerations we will assume that modes with higher momentum than the observable CMB modes are not excited. The highest momentum excited mode therefore satisfies

$$p_{\rm UV} \geq 10^n H. \tag{3.61}$$

The energy density stored in the fluctuations after adiabatic subtraction

is given by

$$\langle \rho_{\mathcal{R}} \rangle = M_P^2 \epsilon \int_0^\infty \frac{d^3k}{(2\pi)^3} \left[|\dot{\mathcal{R}}_{k,\mathrm{excited}}|^2 - |\dot{\mathcal{R}}_{k,BD}|^2 + \frac{k^2}{a^2} \left(|\mathcal{R}_{k,\mathrm{excited}}|^2 - |\mathcal{R}_{k,BD}|^2 \right) \right], \tag{3.62}$$

We will consider different functional forms of scale dependence for the Bogoliubov parameter $\beta_k = |\beta| f_k$ shown in Table 3.1.

f_k	$\langle \rho_{\mathcal{R}} \rangle$
$\Theta\left(k_{\mathrm{UV}} - k\right)$	$\frac{\lvert\beta\rvert^2}{8\pi^2}\left(p_{\mathrm{UV}}^4 + H^2 p_{\mathrm{UV}}^2\right)$
$\exp[-k/k_{\mathrm{UV}}]$	$\frac{\lvert\beta\rvert^2}{16\pi^2}\left(3p_{\mathrm{UV}}^4 + H^2 p_{\mathrm{UV}}^2\right)$
$\exp[-(k/k_{\mathrm{UV}})^2]$	$\frac{\lvert\beta\rvert^2}{16\pi^2}\left(p_{\mathrm{UV}}^4 + H^2 p_{\mathrm{UV}}^2\right)$

Table 3.1: The energy density for the different functional forms of $\beta_k = |\beta| f_k$ that are considered. The first form is that used in [13, 14, 40, 47]. As emphasized in [23], the oscillations resulting from instant transitions are very rapid so the effective β_k seen by experiments would appear nearly scale invariant. Bounds on the gaussian form were considered in [16, 17, 42, 51].

The energy density stored in the fluctuations should remain sub-dominant to the kinetic energy of the inflaton field, $\epsilon M_P^2 H^2$, in order for $\epsilon_H = \epsilon_\phi$ to remain true. This backreaction bound may be written as

$$\langle \rho_{\mathcal{R}} \rangle < \epsilon M_P^2 H^2 = \frac{H^4}{8\pi^2 A_S} |\alpha_{k_*} + \beta_{k_*}|^2. \tag{3.63}$$

It is convenient to introduce a parameter which is the coefficient ratio for the leading energy density terms in Table 3.1,

$$c_f = \begin{cases} 1, & f_k = \Theta\left(k_{\mathrm{UV}} - k\right) \\ 2/3, & f_k = \exp[-k/k_{\mathrm{UV}}] \\ 2, & f_k = \exp[-(k/k_{\mathrm{UV}})^2] \end{cases} . \tag{3.64}$$

The backreaction bound gives us,

$$p_{\rm UV} \lesssim \frac{H|\alpha_{k_*} + \beta_{k_*}|^{1/2}}{A_S^{1/4}|\beta|^{1/2}} \times c_f^{1/4} \tag{3.65}$$

Recalling that $|\alpha_k|^2 = 1 + |\beta_k|^2$, using (3.61) and (3.65) we obtain an upper bound for $|\beta|$ given by

$$|\beta| \lesssim 10^{-2n} A_S^{-1/2} c_f^{1/2}. \tag{3.66}$$

We provide the numerical evaluation of the $|\beta|$ upper bound and the corresponding bounds on $|\alpha_k + \beta_k|$ in Table 3.2.

f_k	$\lvert\beta\rvert$ UB	$\lvert\alpha_{k_*} + \beta_{k_*}\rvert$ LB	$\lvert\alpha_{k_*} + \beta_{k_*}\rvert$ UB
$\Theta\left(k_{\rm UV} - k\right)$	0.022	0.97	1.022
$\exp[-k/k_{\rm UV}]$	0.018	0.98	1.02
$\exp[-(k/k_{\rm UV})^2]$	0.031	0.97	1.03

Table 3.2: Bounds on $\beta_k = |\beta| f_k$ and $|\alpha_k + \beta_k|$ arising from backreaction considerations. We have taken $n = 3$ and $k_* = 0.05$ Mpc$^{-1} \sim 0.5 k_{\rm UV}$ for the numerical estimates. To obtain the lower bound we have allowed β_k to be negative.

3.5.2 Bounds from the measurement of n_s

As reported in Table 2.1, the scalar spectral index n_s has been measured to a high precision. We will calculate the bound placed on $|\beta|$ from the measurement of n_s using (3.58). For the scale invariant case there is no bound since the contribution to n_s vanishes. For the exponential and the gaussian cases of f_k we find non-vanishing contributions.

To obtain an upper bound on $|\beta|$, assume that $n_{s,\rm BD} \approx 1$. This is equivalent to saying that the deviation from scale invariance arises due to the

excited state parameters. We present upper bound for $|\beta|$ in Table 3.3. These bounds are subdominant to the backreaction bounds previously obtained.

f_k	$\|\beta\|$ UB	$\|\alpha_k + \beta_k\|$ LB	$\|\alpha_k + \beta_k\|$ UB
$\exp[-k/k_{\rm UV}]$	0.06	0.96	1.04
$\exp[-(k/k_{\rm UV})^2]$	0.05	0.96	1.04

Table 3.3: The numerical bounds on $|\beta|$ and $|\alpha_k + \beta_k|$ for different functional forms of $\beta_k = |\beta| f_k$. We have taken $k \sim 0.5 k_{\rm UV}$ for numerical estimates.

3.5.3 Bounds from observational limits on $f_{\rm NL}^{\rm loc}$

From our discussion of excitation bounds arising from backreaction considerations and the measurement of n_s we know that $|\beta| \ll 1$. We have previously computed the leading contribution to $f_{\rm NL}^{\rm loc}$ in the $|\beta| < 1$ regime (3.57),

$$f_{\rm NL}^{\rm loc} \approx \frac{10}{3}\epsilon \left(\frac{k_{\rm S}}{k_{\rm L}}\right) {\rm Re}\left[\beta_{k_{\rm S}}\right]. \tag{3.67}$$

The most aggressive bound which may be formed is given by $(k_S/k_L) \approx 10^3$ and $\epsilon \approx 10^{-3}$. Since we have a 1σ upper bound of 5.8 (see Table 2.1), we obtain the bound

$$|\beta| \lesssim 5.8 \left(\frac{3}{10}\right)\left(\frac{k_L}{k_S}\right)\frac{1}{\epsilon} \approx 1.8. \tag{3.68}$$

However, since we already have concluded that $|\beta|$ should be less than unity due to previous considerations this upper bound is too weak to be of practical use.

3.5.4 Special case: only $l \lesssim 30$ modes excited

For the lowest l cosmic variance limited modes ($l \lesssim 30$), one may not use scale invariance to bound the excitation amplitude. Instead, we compare the theoretical prediction with the observational error bar width [1] to obtain a conservative estimate of $0.5 \lesssim |\alpha_k + \beta_k|^2 \lesssim 2$.

Chapter 4

Mechanisms

Thus far we have taken for granted that it is possible for excited initial states to exist and have discussed the observational implications of their existence. In this chapter we present a concrete construction of a physical mechanism capable of generating excited initial states.[1]

The basic approach taken here is to change the equation of state parameter, w, in such a way as to excite the field. Since a change in the equation of state parameter corresponds to a change in the slow roll parameter ϵ, there is an additional friction term in the equation of motion for scalar perturbations which is not present for tensor perturbations as we have discussed in section 2.4.

We will explicitly study how the equation of state parameter evolves as a function of time. In section 4.1 we will study case of an instant transition in time. This is an idealized case, but it is useful since the spectrum of excitations may be computed analytically. In section 4.2 we will model the time dependence of the equation of state parameter transition with a hyperbolic tangent. By relating the spectrum of excitations found in these sections to the

[1]The results in this chapter are based on [15].

bounds on excitation amplitude obtained previously, we be able to bound the parameters of the transition.

4.1 Instant transitions

The idealized case of an instantaneous transition from one equation of state parameter value to a different value is useful since it allows for an analytical calculation of the excited spectrum. We will later discuss the case of a gradual transition and how well the excited spectrum from a gradual transition is modeled by the idealized case. Figure 4.1 illustrates the transition for two different values of w_0.

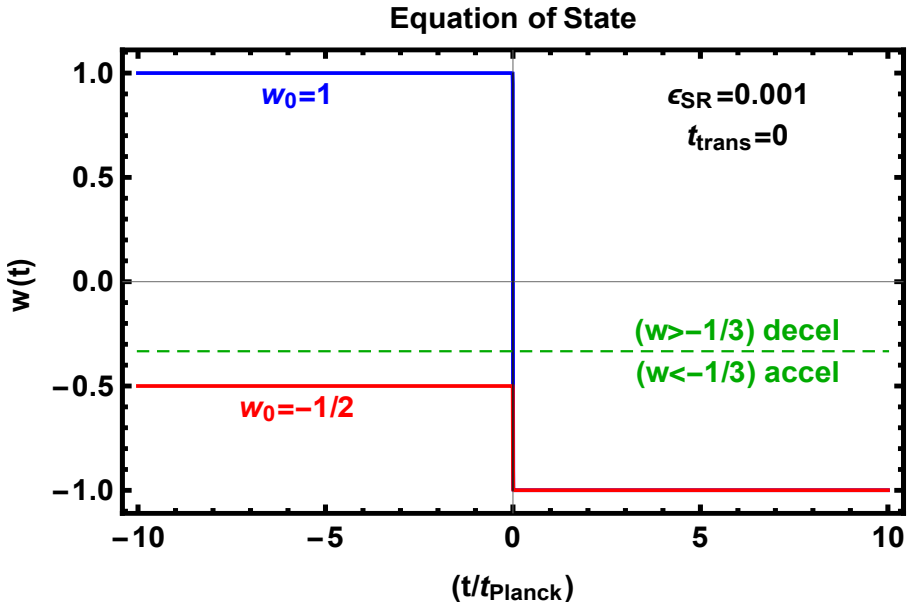

Figure 4.1: Examples of instantaneous transitions.

4.1.1 Matching conditions

The instant transitions that we are considering effectively have a discontinuity in the slow roll parameter ϵ. Therefore, one must be careful when determining which quantities related to $\mathcal{R}$ are continuous since the evolution of $\mathcal{R}$ depends explicitly on $\dot{\epsilon}$ according to (2.50). It was emphasized in [23, 31] that the proper matching conditions are given by

$$[\mathcal{R}_k]_\pm = 0, \quad \left[\epsilon\dot{\mathcal{R}}_k\right]_\pm = 0, \tag{4.1}$$

where we have used the notation that $[\cdots]_\pm$ denotes the change in a quantity across the transition. The origin of these conditions may be easily seen from the differential equation for scalar fluctuations (2.50), which can be rewritten as

$$\frac{d}{dt}\left(a^3\epsilon\dot{\mathcal{R}}_k\right) = -k^2 a\epsilon\mathcal{R}_k. \tag{4.2}$$

The fluctuation mode function itself, $\mathcal{R}_k$, is continuous. If we note that $\epsilon = d(1/H)/dt$, we may time integrate both sides of the equation close to the transition to obtain the continuity condition on the derivative of the mode function,

$$\left[a^3\epsilon\dot{\mathcal{R}}_k\right]_\pm = \lim_{\delta\to 0}\int_{(\Delta t)_t=-\delta}^{(\Delta t)_t=\delta} dt\left(-k^2 a\epsilon\mathcal{R}_k\right) = \left[-k^2\frac{a}{H}\mathcal{R}_k\right]_\pm = 0. \tag{4.3}$$

We have introduced the notation $(\Delta t)_t = (t - t_{\rm trans})$ to denote that time difference between the cosmic time and the time of transition.

Microscopically, the inflaton field will take on a uniform value[2] at the

[2]Note that $\delta\phi = 0$ in the comoving gauge [64].

transition time $(\Delta t)_t = 0$. This implies in the language of [23, 31] that the transition is characterized by a spacetime hypersurface of constant field value, which directly yields (4.1). This is in contrast to the examples studied in [31] in which the transition was characterized by a surface of constant energy density and hence the uniform density gauge is more appropriate since $\delta\rho = 0$ in that gauge. The continuity conditions (4.1) have been verified numerically by time evolving (2.50).

4.1.2 Observables: allowed parameter space

Based on the matching conditions previously discussed, we would like to solve the following system of equations:

$$\begin{aligned} (\Delta t)_t = 0: \quad & \alpha_{0,k}\mathcal{R}_{0,k} + \beta_{0,k}\mathcal{R}^*_{0,k} &&= && \alpha_{f,k}\mathcal{R}_{\mathrm{SR},k} + \beta_{f,k}\mathcal{R}^*_{\mathrm{SR},k}, \\ (\Delta t)_t = 0: \quad & \epsilon_0\left(\alpha_{0,k}\dot{\mathcal{R}}_{0,k} + \beta_{0,k}\dot{\mathcal{R}}^*_{0,k}\right) &&= && \epsilon_{\mathrm{SR}}\left(\alpha_{f,k}\dot{\mathcal{R}}_{\mathrm{SR},k} + \beta_{f,k}\dot{\mathcal{R}}^*_{\mathrm{SR},k}\right). \end{aligned} \tag{4.4}$$

The explicit forms of the functions $\mathcal{R}_{0,k}$ and $\mathcal{R}_{\mathrm{SR},k}$ are given in (4.8). The coefficients $\{\alpha_{0,k}, \beta_{0,k}\}$ account for the fact that the spectrum may be excited prior to the transition to slow-roll inflation. The case of the lowest energy density vacuum state transitioning to inflation is given by the choice $\alpha_{0,k} = 1$ and $\beta_{0,k} = 0$.

In order to solve (4.4), we must find a solution to scalar fluctuation mode equation which is properly normalized. The normalization condition is given by the canonical commutation relation, which may be rewritten as a condition on the Wronskian (2.55) of the scalar fluctuation mode function as

follows

$$2a^3 M_P^2 \epsilon \left(\dot{\mathcal{R}}_k \mathcal{R}_k^* - \mathcal{R}_k \dot{\mathcal{R}}_k^* \right) = i. \tag{4.5}$$

The background geometry evolution is given by

$$\epsilon = \begin{cases} \epsilon_{\rm SR} & (\Delta t)_t < 0 \\ \epsilon_0 & (\Delta t)_t > 0 \end{cases}, \quad H(t) = H_t \left[1 + \epsilon \, H_t (\Delta t)_t \right]^{-1}, \quad a(t) = a_t \left(\frac{H_t}{H(t)} \right)^{1/\epsilon}. \tag{4.6}$$

We have defined H_t and a_t as the Hubble parameter and scale factor at the time of transition, $(\Delta t)_t = 0$. It is convenient to introduce the variables

$$\begin{aligned} (\Delta t)_t < 0: \quad & \tilde{\tau}_0 = \int \frac{dt}{a} = \frac{1}{(-1+\epsilon_0)} \frac{1}{a(t) H(t)}, \\ (\Delta t)_t > 0: \quad & \tilde{\tau}_{\rm SR} = \int \frac{dt}{a} = \frac{1}{(-1+\epsilon_{\rm SR})} \frac{1}{a(t) H(t)}. \end{aligned} \tag{4.7}$$

The properly normalized solution to the scalar equation of motion (2.50) for a constant equation of state is given as[3]

$$\begin{aligned} (\Delta t)_t < 0: \quad & \mathcal{R}_{0,k}(t) = \sqrt{\frac{\pi}{2^3 \, \epsilon_0}} \frac{1}{M_P \, a(t)} \sqrt{|\tilde{\tau}_0|} \, H^2_{\nu_0} \left[k |\tilde{\tau}_0| \right], \qquad \nu_0 = \frac{3}{2} \frac{(1-w_0)}{(1+3w_0)} \\ (\Delta t)_t > 0: \quad & \mathcal{R}_{{\rm SR},k}(t) = \sqrt{\frac{\pi}{2^3 \, \epsilon_{\rm SR}}} \frac{1}{M_P \, a(t)} \sqrt{|\tilde{\tau}_{\rm SR}|} \, H^2_{\nu_{\rm SR}} \left[k |\tilde{\tau}_{\rm SR}| \right], \quad \nu_{\rm SR} = \frac{3}{2} \frac{(1-w_{\rm SR})}{(1+3w_{\rm SR})} \end{aligned} \tag{4.8}$$

Employing the matching conditions (4.4) we are able to write the Bogoliubov parameters for an arbitrary choice of w_0 and initial excitation parameters α_0 and β_0 as

$$\alpha_{f,k} = \sqrt{\frac{\epsilon_0}{\epsilon_{\rm SR}}} \sqrt{\left| \frac{\epsilon_{\rm SR} - 1}{\epsilon_0 - 1} \right|} \frac{\alpha_{\rm num}}{\alpha_{\rm denom}}, \quad \beta_{f,k} = \alpha_{f,k} \text{ with } H^1_{f(\nu_{\rm SR})} \leftrightarrow H^2_{f(\nu_{\rm SR})}, \tag{4.9}$$

[3]Note that $H^{1,2}_\nu (x \to \infty) \to e^{\pm i x}$.

$$\alpha_{\rm num} = \left(\begin{array}{c} s_{\tau_0} H^1_{\nu_{\rm SR}}(x_{\rm SR}) \left\{ \alpha_0 \left[H^2_{\nu_0-1}(x_0) - H^2_{\nu_0+1}(x_0) \right] + \beta_0 \left[H^1_{\nu_0-1}(x_0) - H^1_{\nu_0+1}(x_0) \right] \right\} \\ + \left[\alpha_0 H^2_{\nu_0}(x_0) + \beta_0 H^1_{\nu_0}(x_0) \right] \left\{ \frac{\epsilon_{\rm SR}}{\epsilon_0} \left[H^1_{\nu_{\rm SR}-1}(x_{\rm SR}) - H^1_{\nu_{\rm SR}+1}(x_{\rm SR}) \right] \right. \\ \left. + \frac{a_t H_t}{k} H^1_{\nu_{\rm SR}}(x_{\rm SR}) \left[-2 \left(1 - \frac{\epsilon_{\rm SR}}{\epsilon_0} \right) + s_{\tau_0} |\epsilon_0 - 1| + \frac{\epsilon_{\rm SR}}{\epsilon_0} |\epsilon_{\rm SR} - 1| \right] \right\} \end{array} \right), \tag{4.10}$$

$$\alpha_{\rm denom} = \left(\begin{array}{c} H^1_{\nu_{\rm SR}}(x_{\rm SR}) \left[H^2_{\nu_{\rm SR}+1}(x_{\rm SR}) - H^2_{\nu_{\rm SR}-1}(x_{\rm SR}) \right] \\ -H^2_{\nu_{\rm SR}}(x_{\rm SR}) \left[H^1_{\nu_{\rm SR}+1}(x_{\rm SR}) - H^1_{\nu_{\rm SR}-1}(x_{\rm SR}) \right] \end{array} \right). \tag{4.11}$$

Here we have defined $x_0 = |\epsilon_0 - 1|^{-1}(k/a_t H_t)$, $x_{\rm SR} = |\epsilon_{\rm SR} - 1|^{-1}(k/a_t H_t)$ and $s_{\tau_0} = \text{sign}(\tilde{\tau}_0)$.

A special case of interest is a transition for which $\alpha_0 = 1$ and $\beta_0 = 0$, corresponding to a transition from the state of lowest energy density prior to the transition. We will concentrate on this case for the remainder of the paper until section 4.3. The Bogoliubov parameters are oscillatory in nature, but in practice the oscillations can not be resolved experimentally and it is appropriate to approximate $\beta_{f,k} \approx \beta_f$.

To clarify what we mean when we state that the oscillations cannot be resolved experimentally, we compare the scale of oscillations to the binning scale used by the Planck experiment [3]. The baseline Plik likelihood bin sizes are $\Delta l = 1$ for $l < 30$, $\Delta l = 5$ for $30 \leq l \leq 99$, $\Delta l = 9$ for $100 \leq l \leq 1503$, $\Delta l = 17$ for $1504 \leq l \leq 2013$ and $\Delta l = 33$ for $2014 \leq l \leq 2508$. The oscillations in $\alpha_{f,k}$ and $\beta_{f,k}$ are controlled by $k\tau_{0,t}$, which results in several oscillations in a $\Delta l = 1$ window.

Having computed the excitation spectrum that results from an instant transition, we can translate the bounds obtained in section 3.5 into bounds on w_0.

From our strongest bounds on $|\beta_f|$ summarized in Table 3.2 and section 3.5.4, we may tabulate the largest allowed w_0 for a given $\epsilon_{\rm SR}$. Consider the effect of $\beta_0 = |\beta_0| \exp(i\theta_0)$. We see from Figure 4.2 that $|\alpha_f + \beta_f|$ is maximal for $\{|\beta_0|, \theta_0\} = \{\text{large}, 0\}$ and minimal for $\{|\beta_0|, \theta_0\} = \{\text{large}, \pi\}$. Since we have identified both an upper and lower bound on $|\alpha_f + \beta_f|$, we will take the intermediate case of $\alpha_0 = 1$ and $\beta_0 = 0$. In Table 4.1 we present the bounds on the fractional change of w and ϵ.

Observed Multipoles Excited	Relevant Bound	$100\lvert\frac{w_0 - w_{\rm SR}}{w_{\rm SR}}\rvert$	$100\lvert\frac{\epsilon_0 - \epsilon_{\rm SR}}{\epsilon_{\rm SR}}\rvert$
$l \lesssim 30$	$0.71 \lesssim \lvert\alpha_{f,k} + \beta_{f,k}\rvert \lesssim 1.41$	$\lesssim 0.07$	$\lesssim 94$
$l > 30$ and lower	$0.97 < \lvert\alpha_{f,k} + \beta_{f,k}\rvert < 1.022$	$\lesssim 0.003$	$\lesssim 4.3$

Table 4.1: The maximal allowed ϵ_0 for a given $\epsilon_{\rm SR} < \epsilon_0$. We have reported the bounds for $\epsilon_{\rm SR} = 10^{-3}$, though we have confirmed that the bound on the fractional change of ϵ is not numerically sensitive to this input. We have chosen $\alpha_0 = 1$ and $\beta_0 = 0$.

If the transition to inflation is well approximated as an instantaneous transition with an initial w_0 larger than is stated in Table 4.1, the modes which are excited cannot comprise our observable CMB. Note that modes which are super-Planckian at the time of transition should be described by the Bunch-Davies vacuum when their momenta redshift to become sub-Planckian in order for the stress-energy tensor to be renormalizable [23].

We note for completeness that the bounds on the fractional change in

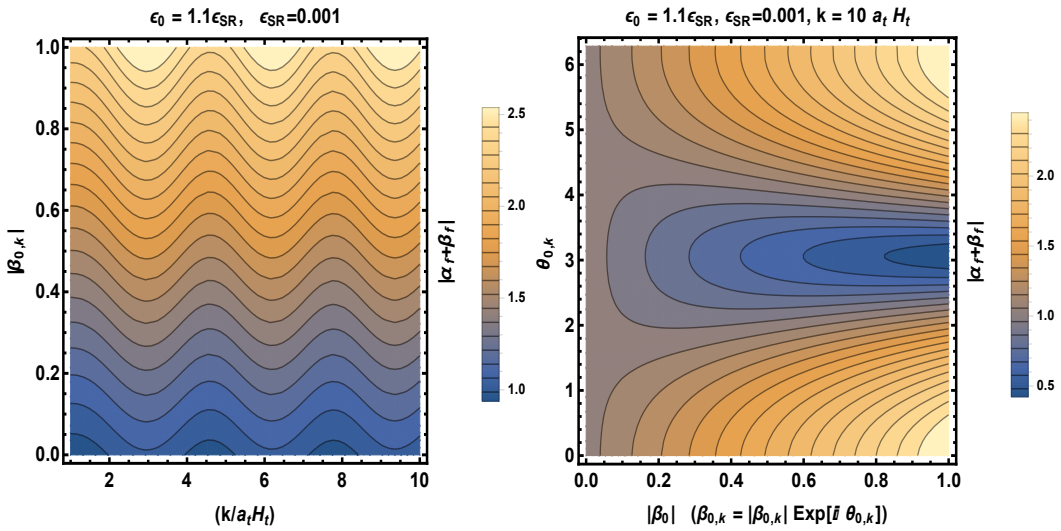

Figure 4.2: Amplitude of excitations $|\alpha_{f,k} + \beta_{f,k}|$ after transition for initially excited state with $\beta_{0,k} \neq 0$. We have taken the form of the excitation prior to the transition to be $\beta_{0,k} = |\beta_{0,k}| \exp(i\theta_{0,k})$ for arbitrary $\theta_{0,k}$ in the right plot and $\theta_{0,k} = 0$ in the left plot. These plots indicate that a larger $|\beta_{0,k}|$ typically leads to a larger deviation of $|\alpha_{f,k} + \beta_{f,k}|$ from unity. This justifies our choice of $\beta_{0,k} = 0$ to derive our bounds presented in Table 4.1.

ϵ are more restrictive if we consider a transition in which ϵ increases. The bounds are explicitly given in Table 4.2. In Figure 4.5 we demonstrate how the morphology of the spectrum changes depending on whether the step in ϵ is to a smaller or larger ϵ.

4.1.3 Comparison with Previous Work

There have been many previous studies analyzing equation of state transitions [7, 13, 21, 23, 27, 25, 28, 30]. Some recent examples with which we could easily compare our matching criteria are [21, 25, 27, 28, 30]. The matching conditions used in those studies do not agree with the matching con-

Observed Multipoles Excited	Relevant Bound	$100\lvert\frac{w_0-w_{\rm SR}}{w_{\rm SR}}\rvert$	$100\lvert\frac{\epsilon_0-\epsilon_{\rm SR}}{\epsilon_{\rm SR}}\rvert$
$l \lesssim 30$	$0.71 \lesssim \lvert\alpha_{f,k}+\beta_{f,k}\rvert \lesssim 1.41$	$\lesssim 0.03$	$\lesssim 43$
$l > 30$ and lower	$0.97 < \lvert\alpha_{f,k}+\beta_{f,k}\rvert < 1.022$	$\lesssim 0.003$	$\lesssim 3.3$

Table 4.2: The maximal allowed ϵ_0 for a given $\epsilon_{\rm SR} > \epsilon_0$. We have reported the bounds for $\epsilon_{\rm SR} = 10^{-3}$, though we have confirmed that the bound on the fractional change of ϵ is not numerically sensitive to this input. We have chosen $\alpha_0 = 1$ and $\beta_0 = 0$.

ditions presented in equation (4.1). We also note that studies which numerically evolve the Muhkanov-Sasaki equation without making approximations for $\{\dot{z}, \ddot{z}\}$ should yield the correct result if a proper step size is chosen so that the transition is sampled.

One of our conclusions is that only transitions from one inflationary phase to another are allowed to be imprinted on the observable CMB. A special case which has been studied previously is steps in the inflationary potential which are modeled by a hyperbolic tangent of the field value [7]. We find that even for the most violent case of an instant transition with a step size $|\Delta V|/V_0 = \epsilon_0/3$, the fractional change in ϵ almost satisfies our least restrictive bound presented in Table 4.2. To see this explicitly, note that the initial kinetic energy is given by $K_0 = |\Delta V|$ and therefore $K_f = 2K_0$ by energy conservation. The fractional change in $\epsilon \approx 3K/V$ is given by

$$\epsilon_0 = \frac{1}{2}\frac{\epsilon_{\rm SR}}{(1+\epsilon_{\rm SR}/6)} \approx \frac{1}{2}\epsilon_{\rm SR}, \quad \lvert\frac{\epsilon_0-\epsilon_{\rm SR}}{\epsilon_{\rm SR}}\rvert \approx 0.5. \tag{4.12}$$

4.2 Gradual transitions

4.2.1 Transition model

Our parameterization of the gradual transition is of the form

$$w(t) = w_0 + \frac{1}{2}(w_{\rm SR} - w_0)\left(1 + \tanh\left[\sigma(\Delta t)_t\right]\right), \; w_{\rm SR} = -1 + \frac{2}{3}\epsilon_{\rm SR}. \qquad (4.13)$$

Figure 4.3 illustrates the transition for two different values of w_0 and σ.

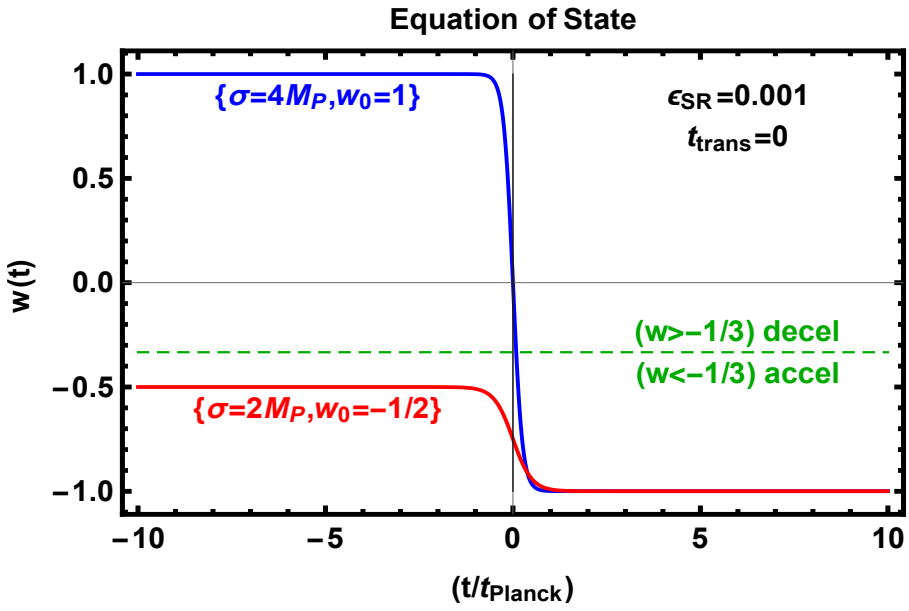

Figure 4.3: The equation of state parameter evolution as a function of the cosmic time in units of the Planck time. The equation of state is given by (4.13).

We have denoted the difference between the cosmic time and the time of transition by $(\Delta t)_t = (t - t_{\rm trans})$. The corresponding $\epsilon(t)$ and $H(t)$ from (1.18) are given by

$$\epsilon(t) = \frac{3}{2}(1+w) = \frac{1}{2}\left(\epsilon_{SR} + \epsilon_0 + (\epsilon_{SR} - \epsilon_0)\tanh\left[\sigma(\Delta t)_t\right]\right), \qquad (4.14)$$

$$H(t) = \frac{H_t}{1 + \frac{1}{2} H_t (\Delta t)_t (\epsilon_0 + \epsilon_{SR}) + \frac{1}{2} \frac{H_t}{\sigma} (\epsilon_{SR} - \epsilon_0) \log\left[\cosh\left[\sigma (\Delta t)_t\right]\right]}. \quad (4.15)$$

In the two limits of $(\Delta t)_t$ large of either sign, the scale factor evolution may be solved analytically

$$a(t) = a_t \times \begin{cases} \left[\frac{1 + \frac{1}{2} H_t (\Delta t)_t (\epsilon_{SR} + \epsilon_0) + \frac{1}{2} \frac{H_t}{\sigma} (\epsilon_{SR} - \epsilon_0) \log\left[\frac{1}{2} e^{\sigma (\Delta t)_t}\right]}{1 - \frac{1}{2} \frac{H_t}{\sigma} (\epsilon_{SR} - \epsilon_0) \log(2)}\right]^{1/\epsilon_{SR}} & , (\Delta t)_t \gg 1 \\ \left[1 + \frac{1}{2} H_t (\Delta t)_t (\epsilon_{SR} + \epsilon_0)\right]^{2/(\epsilon_0 + \epsilon_{SR})} & , (\Delta t)_t \approx 0 \\ \left[\frac{1 + \frac{1}{2} H_t (\Delta t)_t (\epsilon_{SR} + \epsilon_0) + \frac{1}{2} \frac{H_t}{\sigma} (\epsilon_{SR} - \epsilon_0) \log\left[\frac{1}{2} e^{-\sigma (\Delta t)_t}\right]}{1 - \frac{1}{2} \frac{H_t}{\sigma} (\epsilon_{SR} - \epsilon_0) \log(2)}\right]^{1/\epsilon_0} & , (\Delta t)_t \ll 1 \end{cases} . \quad (4.16)$$

The full scale factor evolution must be solved numerically.

4.2.2 Observables: allowed parameter space

The gradual transition has three cases for modes depending on whether a mode experiences the transition as sudden, adiabatic or an intermediate case between the two. For an example of these three regimes, see Figure 4.4. We have explicitly compared the spectrum morphology for a case of transitioning to a lower ϵ to the case of transitioning to a higher ϵ in Figure 4.5.

Comparing the $\dot{\epsilon}$ friction term and the frequency term in the equation of motion (2.50) provides an intuition for the three cases. This is most easily done by rescaling the curvature perturbation in order to eliminate the friction term altogether. The appropriate rescaling is given by

$$\mathcal{R}_k = (a^3\, \epsilon)^{-1/2}\, \bar{\mathcal{R}}_k. \quad (4.17)$$

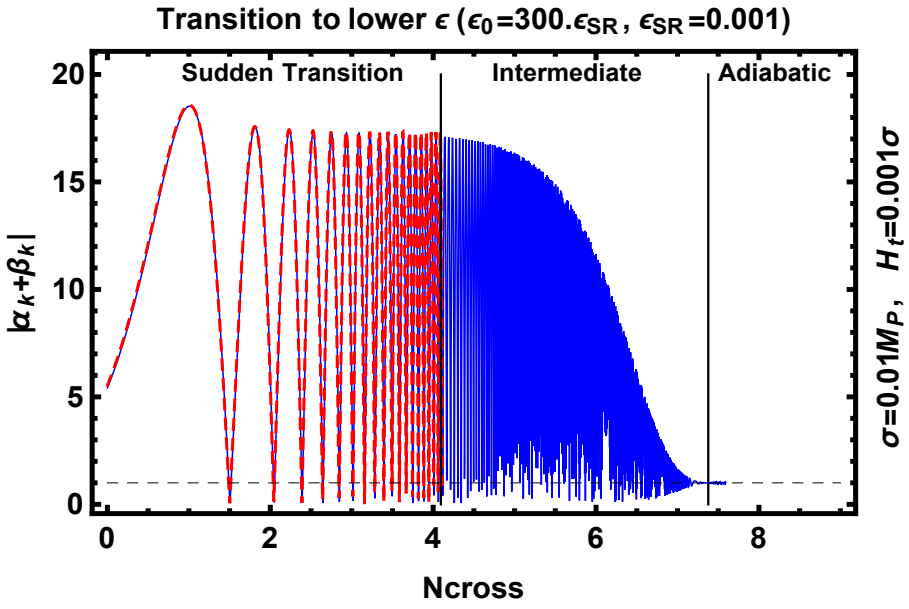

Figure 4.4: A comparison of the spectrum enhancement obtained from the numerical solution (solid blue line) and the analytical formula (dashed red line) obtained from equation (4.9). The parameter $N_{\rm cross} = \log(k/a_t H_t)$ is the number of efolds from the time of the transition until the mode exits the horizon. For the sake of clarity, we end the analytically obtained line at 4 efolds. The numerical solution stops at slightly over 7.5 efolds. The separators between the three regimes of modes are approximately placed.

The resulting rescaled equation of motion is given by

$$\ddot{\bar{\mathcal{R}}}_k + \bar{\omega}_k^2 \bar{\mathcal{R}}_k = 0, \quad \bar{\omega}_k^2 = \left[\left(\frac{k}{a}\right)^2 - \left(\frac{9}{4}H^2 + \frac{3}{2}H\frac{\dot{\epsilon}}{\epsilon} - \frac{1}{4}\frac{\dot{\epsilon}^2}{\epsilon^2}\right) - \frac{1}{2}\left(3\dot{H} + \frac{\ddot{\epsilon}}{\epsilon}\right)\right]. \tag{4.18}$$

Modes for which the term proportional to k dominates the effective frequency $\bar{\omega}_k$ tend to be adiabatic since they satisfy $|\dot{\bar{\omega}}_k/\bar{\omega}_k^2| \ll 1$ during the transition. Likewise, modes which satisfy $|\dot{\bar{\omega}}_k/\bar{\omega}_k^2| \gg 1$ during the transition tend to experience a sudden transition. We summarize these behaviors in Table 4.3.

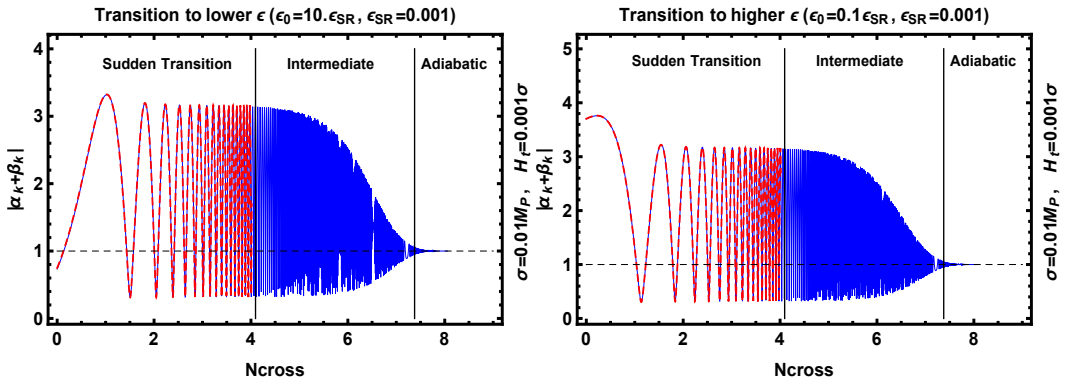

Figure 4.5: Spectrum morphology comparison for a transition to a higher ϵ versus a transition to a lower ϵ. Note that a transition with $\epsilon_0 > \epsilon_{\rm SR}$ tends to reach its first peak for higher momenta than the case of $\epsilon_0 < \epsilon_{\rm SR}$. The separators between the three regimes of modes are approximately placed.

Condition	Cases
$\lvert\dot{\bar{\omega}}_k/\bar{\omega}_k^2\rvert \gg 1$	Sudden Transition
	Intermediate Modes
$\lvert\dot{\bar{\omega}}_k/\bar{\omega}_k^2\rvert \ll 1$	Adiabatic

Table 4.3: Three cases for a given momentum mode depending on how deep inside of the horizon it is during the transition.

From Figure 4.4 there are clearly two distinct cases in which we may observe excited modes:

1. We observe sudden/intermediate modes with an amplitude close to the maximum amplitude, in which case the fractional change in ϵ is strongly bounded (see Table 4.1).

2. We observe only intermediate modes at the low amplitude tail of the spectrum, in which case the fractional change in ϵ may have been large but the modes with a large amplitude are hidden outside of our horizon.

The second case may allow for large fractional change in ϵ compared to the bounds presented in Table 4.1, but it requires fine tuning to ensure that the large amplitude modes are not observed. The fine tuning becomes more concerning as the fractional change in ϵ increases, because difference in amplitude between the hidden modes and the visible modes increases dramatically. Moreover, it is not clear we would be able to infer ϵ_0 from the observation of the low amplitude tail modes.

4.3 Implications for $(20 \lesssim l \lesssim 30)$ power suppression

Observationally there is a suppression of power for multipoles of $20 \lesssim l \lesssim 30$ [3]. A brief discussion of the history associated with discovering and modeling this anomaly is contained in [27]. The observed power suppression is approximately given by

$$\frac{\Delta^2_{\mathcal{R}}|_{\text{expected } 20<l<30}}{\Delta^2_{\mathcal{R}}|_{\text{actual } 20<l<30}} \approx \frac{600}{1000} = 60\%. \tag{4.19}$$

To suppress the scalar power spectrum on large scales, one would need the scale dependence of $|\alpha_k + \beta_k|$ to suppress power for the relevant multipoles.

Based on our discussion in the previous section, there are two possibilities:

1. Sudden transition modes comprise the entire CMB, in which case the bounds from Table 4.1 hold.

2. Only the lowest l modes are excited.

For the first case the largest relative suppression that may be obtained is

$$\frac{|\alpha_k + \beta_k|^2_{LB}}{|\alpha_k + \beta_k|^2_{UB}} \approx \left(\frac{0.97}{1.022}\right)^2 = 90\%, \tag{4.20}$$

This is an insufficient amount of suppression.

For the second case we note that the envelope of the excited spectrum typically monotonically decays from a large excitation amplitude to a smaller excitation amplitude as is depicted in Figure 4.4. Since the modes between $l \approx 10$ and $l \approx 20$ do not show a power suppression to the same extent that the $20 \lesssim l \lesssim 30$ modes do, we do not think that the transitions which we have studied are good candidates for explaining the power suppression anomaly. It may be possible to finely tune the pre-transition excitation parameter $\beta_{0,k}$ (see Figure 4.2) to obtain the desired spectrum, but it is not obvious what mechanism could give rise to such a selected excitation.

Chapter 5

Conclusions

Inflationary cosmology provides a framework for connecting the cosmological parameters to an underlying microscopic theory. We have reviewed the motivations and formulation of inflationary theory. Cosmological perturbation theory was introduced and used to connect the cosmological parameters to the dynamics of the inflaton field. The physics of inflationary initial states which are excited has been discussed and the observational consequences were presented. We derived bounds on the excitation amplitude of initial states from observational consistency arguments. Furthermore, we have studied how transitions generate excited initial states and mapped the excitation bounds onto bounds for the parameters of the transition.

We have revisited the physics of early universe transitions to slow-roll inflation. The proper matching conditions must be used when determining the spectrum of excited fluctuations across an equation of state transition. A careful numerical study of the problem agrees with matching $\left\{\mathcal{R}, \epsilon\dot{\mathcal{R}}\right\}$ as opposed to $\left\{\mathcal{R}, \dot{\mathcal{R}}\right\}$. There are three regimes present in a gradual transition: modes which experience a sudden transition, adiabatic modes and modes which interpolate between those two regimes which we call intermediate modes.

If the modes comprising the visible CMB contain imprints of the transition, we have shown that the pre-transition universe must likewise be an inflationary period. The only exception is if the very low l modes are comprised of intermediate modes generated by a transition from a large w_0. We have also argued that is it very unlikely that equation of state transitions can explain the low multipole power suppression observed in the CMB since it requires a very localized excitation in momentum space prior to the transition.

Our results state that the physics which preceded inflation is not likely to be imprinted on the observable CMB. This is a discouraging result from the perspective of using CMB observations to gain insight into the earliest stages of our universe. However, it is encouraging since it allows us to interpret cosmological observations in the context of inflationary cosmology without having to worry about potential ambiguities introduced by pre-inflationary physics.

Bibliography

[1] R. Adam et al. Planck 2015 results. I. Overview of products and scientific results. 2015.

[2] P. A. R. Ade et al. Planck 2013 Results. XXIV. Constraints on primordial non-Gaussianity. *Astron. Astrophys.*, 571:A24, 2014.

[3] P. A. R. Ade et al. Planck 2015 results. XIII. Cosmological parameters. 2015.

[4] P. A. R. Ade et al. Planck 2015 results. XVII. Constraints on primordial non-Gaussianity. 2015.

[5] P. A. R. Ade et al. Planck 2015 results. XX. Constraints on inflation. 2015.

[6] P. A. R. Ade et al. Improved Constraints on Cosmology and Foregrounds from BICEP2 and Keck Array Cosmic Microwave Background Data with Inclusion of 95 GHz Band. *Phys. Rev. Lett.*, 116:031302, 2016.

[7] Peter Adshead, Cora Dvorkin, Wayne Hu, and Eugene A. Lim. Non-Gaussianity from Step Features in the Inflationary Potential. *Phys. Rev.*, D85:023531, 2012.

[8] Peter Adshead, Richard Easther, and Eugene A. Lim. The 'in-in' Formalism and Cosmological Perturbations. *Phys. Rev.*, D80:083521, 2009.

[9] Ivan Agullo and Leonard Parker. Non-gaussianities and the Stimulated creation of quanta in the inflationary universe. *Phys. Rev.*, D83:063526, 2011.

[10] Andreas Albrecht, Pedro Ferreira, Michael Joyce, and Tomislav Prokopec. Inflation and squeezed quantum states. *Phys. Rev.*, D50:4807–4820, 1994.

[11] R. A. Alpher, H. Bethe, and G. Gamow. The Origin of Chemical Elements. *Physical Review*, 73:803–804, April 1948.

[12] Luca Amendola et al. Cosmology and fundamental physics with the Euclid satellite. *Living Rev. Rel.*, 16:6, 2013.

[13] Aditya Aravind, Dustin Lorshbough, and Sonia Paban. Non-Gaussianity from Excited Initial Inflationary States. *JHEP*, 07:076, 2013.

[14] Aditya Aravind, Dustin Lorshbough, and Sonia Paban. Bogoliubov Excited States and the Lyth Bound. *JCAP*, 1408:058, 2014.

[15] Aditya Aravind, Dustin Lorshbough, and Sonia Paban. On primordial equation of state transitions. 2016.

[16] Amjad Ashoorioon, Konstantinos Dimopoulos, M. M. Sheikh-Jabbari, and Gary Shiu. Non-Bunch–Davis initial state reconciles chaotic models with BICEP and Planck. *Phys. Lett.*, B737:98–102, 2014.

[17] Amjad Ashoorioon, Konstantinos Dimopoulos, M. M. Sheikh-Jabbari, and Gary Shiu. Reconciliation of High Energy Scale Models of Inflation with Planck. *JCAP*, 1402:025, 2014.

[18] Neil Barnaby, Jordan Moxon, Ryo Namba, Marco Peloso, Gary Shiu, and Peng Zhou. Gravity waves and non-Gaussian features from particle production in a sector gravitationally coupled to the inflaton. *Phys. Rev.*, D86:103508, 2012.

[19] C. L. Bennett et al. Nine-Year Wilkinson Microwave Anisotropy Probe (WMAP) Observations: Final Maps and Results. *Astrophys. J. Suppl.*, 208:20, 2013.

[20] N. D. Birrell and P. C. W. Davies. *Quantum Fields in Curved Space*. Cambridge Monographs on Mathematical Physics. Cambridge Univ. Press, Cambridge, UK, 1984.

[21] Yong Cai, Yu-Tong Wang, and Yun-Song Piao. Preinflationary primordial perturbations. *Phys. Rev.*, D92(2):023518, 2015.

[22] Esteban A. Calzetta and Bei-Lok B. Hu. *Nonequilibrium Quantum Field Theory*. Cambridge University Press, 2008.

[23] Daniel Carney, Willy Fischler, Sonia Paban, and Navin Sivanandam. The Inflationary Wavefunction and its Initial Conditions. *JCAP*, 1212:012, 2012.

[24] Sean M. Carroll. *Spacetime and geometry: An introduction to general relativity.* 2004.

[25] Pisin Chen and Yu-Hsiang Lin. What initial condition of inflation would suppress the large-scale CMB spectrum? *Phys. Rev.*, D93(2):023503, 2016.

[26] Xingang Chen, Min-xin Huang, Shamit Kachru, and Gary Shiu. Observational signatures and non-Gaussianities of general single field inflation. *JCAP*, 0701:002, 2007.

[27] Michele Cicoli, Sean Downes, Bhaskar Dutta, Francisco G. Pedro, and Alexander Westphal. Just enough inflation: power spectrum modifications at large scales. *JCAP*, 1412(12):030, 2014.

[28] Carlo R. Contaldi, Marco Peloso, Lev Kofman, and Andrei D. Linde. Suppressing the lower multipoles in the CMB anisotropies. *JCAP*, 0307:002, 2003.

[29] Paolo Creminelli, Diana L. López Nacir, Marko Simonović, Gabriele Trevisan, and Matias Zaldarriaga. Detecting Primordial B-Modes after Planck. *JCAP*, 1511(11):031, 2015.

[30] Suratna Das, Gaurav Goswami, Jayanti Prasad, and Raghavan Rangarajan. Revisiting a pre-inflationary radiation era and its effect on the CMB power spectrum. *JCAP*, 1506(06):001, 2015.

[31] Nathalie Deruelle and Viatcheslav F. Mukhanov. On matching conditions for cosmological perturbations. *Phys. Rev.*, D52:5549–5555, 1995.

[32] R. H. Dicke, P. J. E. Peebles, P. G. Roll, and D. T. Wilkinson. Cosmic Black-Body Radiation. *APJ*, 142:414–419, July 1965.

[33] Scott Dodelson and Lam Hui. A Horizon ratio bound for inflationary fluctuations. *Phys. Rev. Lett.*, 91:131301, 2003.

[34] William E. East, Matthew Kleban, Andrei Linde, and Leonardo Senatore. Beginning inflation in an inhomogeneous universe. 2015.

[35] Stefan Eccles, Willy Fischler, Dustin Lorshbough, and Benjamin A. Stephens. Vector field instability and the primordial tensor spectrum. 2015.

[36] Rhodri Evans. *The Cosmic Microwave Background. How It Changed Our Understanding of the Universe.* Springer, Heidelberg, 2015.

[37] Ricardo Z. Ferreira, Jonathan Ganc, Jorge Noreña, and Martin S. Sloth. On the validity of the perturbative description of axions during inflation. 2015.

[38] Ricardo Z. Ferreira and Martin S. Sloth. Universal Constraints on Axions from Inflation. *JHEP*, 12:139, 2014.

[39] F. Finelli and Robert H. Brandenberger. Parametric amplification of metric fluctuations during reheating in two field models. *Phys. Rev.*, D62:083502, 2000.

[40] Raphael Flauger, Daniel Green, and Rafael A. Porto. On squeezed limits in single-field inflation. Part I. *JCAP*, 1308:032, 2013.

[41] G. Gamow. Expanding Universe and the Origin of Elements. *Physical Review*, 70:572–573, October 1946.

[42] Jonathan Ganc. Calculating the local-type fNL for slow-roll inflation with a non-vacuum initial state. *Phys. Rev.*, D84:063514, 2011.

[43] Juan Garcia-Bellido and David Wands. Constraints from inflation on scalar - tensor gravity theories. *Phys. Rev.*, D52:6739–6749, 1995.

[44] Massimo Giovannini. *A primer on the physics of the cosmic microwave background*. 2008.

[45] Jinn-Ouk Gong and Misao Sasaki. Squeezed primordial bispectrum from general vacuum state. *Class. Quant. Grav.*, 30:095005, 2013.

[46] Christopher Gordon, David Wands, Bruce A. Bassett, and Roy Maartens. Adiabatic and entropy perturbations from inflation. *Phys. Rev.*, D63:023506, 2001.

[47] Brian R. Greene, Koenraad Schalm, Gary Shiu, and Jan Pieter van der Schaar. Decoupling in an expanding universe: Backreaction barely constrains short distance effects in the CMB. *JCAP*, 0502:001, 2005.

[48] Alan H. Guth. The Inflationary Universe: A Possible Solution to the Horizon and Flatness Problems. *Phys. Rev.*, D23:347–356, 1981.

[49] Alan H. Guth. *The inflationary universe: The quest for a new theory of cosmic origins*. 1997.

[50] Alan H. Guth. Eternal inflation and its implications. *J. Phys.*, A40:6811–6826, 2007.

[51] R. Holman and Andrew J. Tolley. Enhanced Non-Gaussianity from Excited Initial States. *JCAP*, 0805:001, 2008.

[52] Paul Hunt and Subir Sarkar. Reconstruction of the primordial power spectrum of curvature perturbations using multiple data sets. *JCAP*, 1401:025, 2014.

[53] Paul Hunt and Subir Sarkar. Search for features in the spectrum of primordial perturbations using Planck and other datasets. *JCAP*, 1512(12):052, 2015.

[54] Marc Kamionkowski and Ely D. Kovetz. The Quest for B Modes from Inflationary Gravitational Waves. 2015.

[55] Matthew Kleban and Leonardo Senatore. Inhomogeneous Anisotropic Cosmology. 2016.

[56] Edward W. Kolb and Michael S. Turner. The Early Universe. *Front. Phys.*, 69:1–547, 1990.

[57] Helge S. Kragh. *Conceptions of cosmos: From myths to the accelerating universe. A history of cosmology*. 2007.

[58] Helge S. Kragh and James M. Overduin. *The weight of the vacuum.* Springerbriefs in physics. Springer, Heidelberg, 2014.

[59] Andrew R Liddle and Samuel M Leach. How long before the end of inflation were observable perturbations produced? *Phys. Rev.*, D68:103503, 2003.

[60] Andrew R. Liddle and D. H. Lyth. *Cosmological inflation and large scale structure.* 2000.

[61] Andrei D. Linde. Particle physics and inflationary cosmology. *Contemp. Concepts Phys.*, 5:1–362, 1990.

[62] David H. Lyth and Andrew R. Liddle. *The primordial density perturbation: Cosmology, inflation and the origin of structure.* 2009.

[63] Juan Martin Maldacena. Non-Gaussian features of primordial fluctuations in single field inflationary models. *JHEP*, 05:013, 2003.

[64] Karim A. Malik and David Wands. Cosmological perturbations. *Phys. Rept.*, 475:1–51, 2009.

[65] Pieter Daniel Meerburg, Jan Pieter van der Schaar, and Pier Stefano Corasaniti. Signatures of Initial State Modifications on Bispectrum Statistics. *JCAP*, 0905:018, 2009.

[66] V. Mukhanov. *Physical Foundations of Cosmology.* Cambridge University Press, Oxford, 2005.

[67] Viatcheslav Mukhanov and Sergei Winitzki. *Introduction to quantum effects in gravity*. Cambridge University Press, 2007.

[68] Shinji Mukohyama, Ryo Namba, Marco Peloso, and Gary Shiu. Blue Tensor Spectrum from Particle Production during Inflation. *JCAP*, 1408:036, 2014.

[69] Ryo Namba, Marco Peloso, Maresuke Shiraishi, Lorenzo Sorbo, and Caner Unal. Scale-dependent gravitational waves from a rolling axion. *JCAP*, 1601(01):041, 2016.

[70] Leonard E. Parker and D. Toms. *Quantum Field Theory in Curved Spacetime*. Cambridge Monographs on Mathematical Physics. Cambridge University Press, 2009.

[71] Hiranya V. Peiris and Licia Verde. The Shape of the Primordial Power Spectrum: A Last Stand Before Planck. *Phys. Rev.*, D81:021302, 2010.

[72] A. A. Penzias and R. W. Wilson. A Measurement of Excess Antenna Temperature at 4080 Mc/s. *APJ*, 142:419–421, July 1965.

[73] Sébastien Renaux-Petel. Primordial non-Gaussianities after Planck 2015: an introductory review. *Comptes Rendus Physique*, 16:969–985, 2015.

[74] Dorothea Samtleben, Suzanne Staggs, and Bruce Winstein. The Cosmic microwave background for pedestrians: A Review for particle and nuclear physicists. *Ann. Rev. Nucl. Part. Sci.*, 57:245–283, 2007.

[75] Dominik J. Schwarz and Erandy Ramirez. Just enough inflation. In *On recent developments in theoretical and experimental general relativity, astrophysics and relativistic field theories. Proceedings, 12th Marcel Grossmann Meeting on General Relativity, Paris, France, July 12-18, 2009. Vol. 1-3*, pages 1241–1243, 2009.

[76] Leonardo Senatore, Kendrick M. Smith, and Matias Zaldarriaga. Non-Gaussianities in Single Field Inflation and their Optimal Limits from the WMAP 5-year Data. *JCAP*, 1001:028, 2010.

[77] A. Taruya and Y. Nambu. Cosmological perturbation with two scalar fields in reheating after inflation. *Phys. Lett.*, B428:37–43, 1998.

[78] David H Weinberg, Michael J Mortonson, Daniel J Eisenstein, Christopher Hirata, Adam G Riess, and Eduardo Rozo. Observational probes of cosmic acceleration. *Physics Reports*, 530(2):87–255, 2013.

[79] Steven Weinberg. *The First Three Minutes. A Modern View of the Origin of the Universe.* 1977.

[80] Steven Weinberg. Quantum contributions to cosmological correlations. *Phys. Rev.*, D72:043514, 2005.

[81] Steven Weinberg. Quantum contributions to cosmological correlations. II. Can these corrections become large? *Phys. Rev.*, D74:023508, 2006.

[82] Steven Weinberg. *Cosmology.* 2008.

[83] Steven Weinberg. Ultraviolet Divergences in Cosmological Correlations. *Phys. Rev.*, D83:063508, 2011.

[84] Daisuke Yamauchi, Andrei Linde, Atsushi Naruko, Misao Sasaki, and Takahiro Tanaka. Open inflation in the landscape. *Phys. Rev.*, D84:043513, 2011.

[85] Ogan Özsoy, Kuver Sinha, and Scott Watson. How Well Can We Really Determine the Scale of Inflation? *Phys. Rev.*, D91(10):103509, 2015.